Pharmacological Research 120 (2017) 116–132

Contents lists available at ScienceDirect

Pharmacological Research

journal homepage: www.elsevier.com/locate/yphrs

Invited Review

Vascular endothelial growth factor (VEGF) and VEGF receptor inhibitors in the treatment of renal cell carcinomas

Robert Roskoski Jr.*

Blue Ridge Institute for Medical Research, 3754 Brevard Road, Suite 116, Box 19, Horse Shoe, NC 28742-8814, United States

ARTICLE INFO

Article history:
Received 14 March 2017
Accepted 15 March 2017
Available online 19 March 2017

Chemical compounds studied in this article:
Axitinib: (PubMED CID: 6450551)
Bevacizumab: (PubMED CID: 24801580)
Pozantinib: (PubMED CID: 25102847)
Lenvatinib: (PubMED CID: 9823820)
Pazopanib (PubMED CID: 10113978)
Sorafenib: (PubMED CID: 216239)
Sunitinib: (PubMed CID: 5329102)

Keywords:
Acquired drug resistance
Catalytic spine
K/E/D/D
Protein kinase inhibitor classification
Protein kinase structure
Targeted cancer therapy

ABSTRACT

One Von Hippel-Lindau (*VHL)* tumor suppressor gene is lost in most renal cell carcinomas while the nondeleted allele exhibits hypermethylation-induced inactivation or inactivating somatic mutations. As a result of these genetic modifications, there is an increased production of VEGF-A and pro-angiogenic growth factors in this disorder. The important role of angiogenesis in the pathogenesis of renal cell carcinomas and other tumors has focused the attention of investigators on the biology of VEGFs and VEGFR1–3 and to the development of inhibitors of the intricate and multifaceted angiogenic pathways. VEGFR1–3 contain an extracellular segment with seven immunoglobulin-like domains, a transmembrane segment, a juxtamembrane segment, a protein kinase domain with an insert of about 70 amino acid residues, and a C-terminal tail. VEGF-A stimulates the activation of preformed VEGFR2 dimers by the *auto*-phosphorylation of activation segment tyrosines followed by the phosphorylation of additional protein-tyrosines that recruit phosphotyrosine binding proteins thereby leading to signalling by the ERK1/2, AKT, Src, and p38 MAP kinase pathways. VEGFR1 modulates the activity of VEGFR2, which is the chief pathway in vasculogenesis and angiogenesis. VEGFR3 and its ligands (VEGF-C and VEGF-D) are involved primarily in lymphangiogenesis. Small molecule VEGFR1/2/3 inhibitors including axitinib, cabozantinib, lenvatinib, sorafenib, sunitinib, and pazopanib are approved by the FDA for the treatment of renal cell carcinomas. Most of these agents are type II inhibitors of VEGFR2 and inhibit the so-called DFG-Asp_{out} inactive enzyme conformation. These drugs are steady-state competitive inhibitors with respect to ATP and like ATP they form hydrogen bonds with the hinge residues that connect the small and large protein kinase lobes. Bevacizumab, a monoclonal antibody that binds to VEGF-A, is also approved for the treatment of renal cell carcinomas. Resistance to these agents invariably occurs within one year of treatment and clinical studies are underway to determine the optimal sequence of treatment with these anti-angiogenic agents. The nivolumab immune checkpoint inhibitor is also approved for the second-line treatment of renal cell carcinomas. Owing to the resistance of renal cell carcinomas to cytotoxic drugs and radiation therapy, the development of these agents has greatly improved the therapeutic options in the treatment of these malignancies.

Contents

1. Clinical course of renal cell carcinomas 117
2. Role of the VEGF and VEGFR families in neovascularization 118
   2.1. An overview of new blood vessel formation 118
   2.2. The VEGF family of growth factors 118
   2.3. The VEGF receptors 119

Abbreviations: AS, activation segment; CDR, antibody complementary determining region; CS or C-spine, catalytic spine; CL, catalytic loop; EGFR, epidermal growth factor receptor; FGFR, fibroblast growth factor receptor; GK, gatekeeper; GRL, Gly-rich loop; HIF1α, hypoxia-inducible factor-1α; IgD, immunoglobulin-like domain; JM, juxtamembrane segment; KID, kinase insert domain; PDGFR, platelet-derived growth factor receptor; PKA, protein kinase A; PlGF, placental growth factor; RCC, renal cell carcinoma; RDP, regulatory domain pocket; RS or R-spine, regulatory spine; Sh1, shell residue 1; VEGFR1/2/3, vascular endothelial growth factor receptors 1–3; VHL, Von Hippel-Lindau.

* Corresponding author.
E-mail address: rrj@brimr.org

http://dx.doi.org/10.1016/j.phrs.2017.03.010
1043-6618/

2.3.1. General properties 119
2.3.2. Structures of the VEGFR1/2/3 and FGFR protein kinase domains and the K/E/D/D motif 121
2.3.3. Function of the juxtamembrane segment 123
2.3.4. Function of the kinase insert domain and carboxyterminal tail in signaling 123
2.3.5. Hydrophobic spines in active and dormant protein kinases 124
3. Pharmacological treatment of metastatic renal cell carcinomas 125
3.1. Structure of VEGFR2-drug complexes 125
3.2. Structure of the VEGF-A-bevacizumab complex 128
3.3. Clinical trials 129
4. Epilogue 130
Acknowledgments 130
References 130

1. Clinical course of renal cell carcinomas

Tumors of the kidney arise from cells in its outer portion, or cortex, and from its inner portion, or medulla. Siegel et al. estimated that about 64,000 new cases of kidney cancer will be diagnosed in the United States in 2017 (41,000 men and 23,000 women) and 24,000 people will die of the disease (14,000 men and 10,000 women) [1]. Deaths from cancer of the kidney account for about 2.3% of all cancer-related mortalities in the United States. Symptoms which prompt a person with renal cell carcinoma to seek medical help include flank pain and hematuria; a palpable abdominal mass may be found in physical examination [2]. Other presenting features are nonspecific and include anemia, fatigue, fever, and weight loss. However, more than one-half of the cases are identified by radiographic examination performed for reasons unrelated to the kidney. Renal cell carcinomas produce a diversity of symptoms owing to abnormal hormone production. These entities include hypertension, hypercalcemia (owing to excess tumor production of parathyroid-like peptide), polycythemia (excess erythropoietin production), and hepatic dysfunction. Risk factors for RCC include cigarette smoking as well as chronic renal disease, obesity, and hypertension.

Renal cell carcinomas are grouped into stages I–IV with stage I representing localized disease and stage IV representing disease with wide spread metastasis [3]. Staging is based upon a tumor/node/metastasis (T/N/M) system: T is based upon the size of the primary tumor and the extent of invasion; N reflects the presence or absence of metastasis to regional lymph nodes; and M denotes whether there are distant metastasis. The respective five-year survival rates are as follows: stage I (90%), stage II (80%), stage III (60%), and stage IV (10%) [4]. Fortunately, only one-third of the patients have stage III–IV disease at the time of diagnosis. Sites of metastasis include the adrenal, bones, brain, liver, lungs, and lymph nodes. The main initial treatment for patients with both localized and metastatic disease is surgery. In those patients with metastatic disease, many undergo so-called cytoreductive nephrectomy before drugs are given. In patients without evidence of metastasis, partial or complete nephrectomies are performed. During the past decade, partial nephrectomies have been performed with laproscopic surgery with good results. The presentation of patients with metastasis at the time of diagnosis indicates that additional therapies are needed. Most kidney cancers are radioresistant and do not respond to cytotoxic drugs. Four major categories of drugs are used to treat metastatic, or advanced, renal cell carcinomas: cytokines, immune checkpoint inhibitors, mTOR inhibitors, and small and large molecule drugs that target the VEGF pathways. This review focuses on the inhibition of VEGFR1/2/3 activity.

Renal cell carcinomas are divided into (i) clear cell and (ii) non-clear cell carcinomas [5]. Clear-cell carcinomas are the most common type and account for 70–80% of kidney cancers. As the name indicates, the cytoplasm of these tumors is clear with clusters of these cells surrounded by prominent endothelial networks. Clear-cell tumors arise from the proximal tubular epithelium. In 98% of all clear-cell neoplasms, whether familial (5%) or sporadic (95%), a loss of DNA occurs on the short arm of chromosome 3, a region that harbors the *VHL* (von Hippel-Lindau) tumor suppressor gene. Oftentimes the nondeleted allele of the *VHL* gene exhibits hypermethylation-induced inactivation or inactivating somatic mutations. The VHL protein is involved in the regulation of the hypoxia-inducible factor-1α (HIF1α) [6]. This is a subunit of a heterodimeric transcription factor that is regulated by the concentration of oxygen. VHL leads to the destruction of HIF1α; VHL recognizes and binds to HIF1α only when oxygen is present owing to the post-translational hydroxylation of two proline residues and an asparagine residue within HIF1α. VHL is an E3-ubquitin ligase that catalyzes the ubiquitylation of HIF1α thereby leading to its proteosomal degradation. When the oxygen levels are low or in cases of when the *VHL* gene is mutated, VHL is unable to bind to HIF1α. This allows HIF1α to dimerize with HIF1β and together they activate the transcription of forty or more genes, including those for the VEGF family, erythropoietin, epidermal growth factor (EGF), platelet-derived growth factor (PDGF), glycolytic enzymes, and genes involved in glucose uptake (GLUT1/4). The increased production of VEGF provides the rationale for the treatment of RCC with inhibitors that target the VEGF or VEGFR families.

The non-clear cell renal carcinomas include papillary carcinomas (10–15% of all kidney cancers), chromophobe carcinomas (5%), and collecting duct carcinomas (<1%) [5]. Papillary renal cell carcinomas cells typically display a basophilic cytoplasm; moreover, foamy histiocytes or macrophages occur within the tumor. These malignancies arise from distal convoluted tubules and are made up of cuboidal cells arranged in papillary structures. The stromal cells within the tumor are usually highly vascularized. Unlike clear-cell carcinoma, multiple papillary tumors may arise simultaneously in one or both kidneys. Papillary RCC occurs in both familial and sporadic forms. One familial form is characterized by trisomy 7 and mutated and activated *MET*. MET is a receptor protein-tyrosine kinase that is activated by the hepatocyte growth factor/scatter factor; activation of MET is associated with angiogenesis and a proclivity for metastasis [7,8]. A second familial form of papillary RCC results from inactivating mutations of the Krebs cycle fumarate hydratase (*FH*) gene [4]. The absence of this enzyme may lead to oxidative cellular damage and tumorigenesis. The mutated forms in the sporadic papillary RCC include trisomies 7 and 17 or loss of the Y chromosome in male patients.

Chromophobe carcinomas represent about 5% of renal cell cancers and they are characterized by pale eosinophic cytoplasm with a halo surrounding the nucleus [5]. These cells arise from the intercalated cells of collecting ducts. Owing to the low frequency of metastasis, the clinical outcome of chromophobe carcinomas is much better than that of clear-cell or papillary cancers. Collecting

Table 1
Human VEGF receptor ligands.

Ligand	Gene	UniProt ID	No. of residues in processed isoforms	Comments
VEGF-A[a]	*VEGFA*	P15692	121, 145, 165, 189, 206	$VEGF_{121/165/189}$ are expressed in all vascularized tissues
VEGF-B	*VEGFB*	P49765	167, 186	Expressed in all tissues except liver
VEGF-C	*VEGFC*	P49767	116	Maturation involves removal of residues 1–31, 32–111, and 228–419; widely expressed
VEGF-D	*VEGFD*	O43915	117	Maturation involves removal of residues 1–21, 22–88, and 206–354; highly expressed in heart, lung, and small intestine
PlGF	*PGF*	P49763	131, 152, 203, 224	Expressed chiefly in placenta, but also ischemic tissues and in various tumors

[a] See UniProt ID: P15692 for a list of a dozen additional isoforms that arise from alternative splicing of pre-mRNA, alternative promoter usage, and alternative initiation.

duct carcinomas make up less than 1% of renal neoplasms. Histologically, these tumors exhibit glandular-like structures enmeshed in a fibrous stroma. These tumors characteristically appear in the kidney medulla. Benign kidney tumors including renal papillary adenomas, angiomyolipomas, and oncocytomas that occur in adults as well as the childhood Wilms tumor, or nephroblastoma, are not considered in this review.

2. Role of the VEGF and VEGFR families in neovascularization

2.1. An overview of new blood vessel formation

The circulation is required for transporting oxygen, nutrients, hormones, and growth factors to and the removal of carbon dioxide and catabolites from cells and organs [6]. New blood vessel formation, or neovascularization, is divided into vasculogenesis and angiogenesis. The former is the process of new blood vessel formation from angioblasts that occurs during embryonic development. The latter is the process of new blood vessel formation from preexisting vasculature. Signaling by the VEGF family is required for both of these processes.

Most endothelial cells in adult humans are quiescent with only 1 in every 10,000 endothelial cells undergoing cell division at any given time [9]. However, endothelial cells divide during (i) wound healing, (ii) ovarian corpus luteum formation, and (iii) placental development [6]. Inhibition of angiogenesis represents a potential therapy for disorders with nonphysiologic angiogenesis including (i) age-related macular degeneration of the eye, (ii) diabetic retinopathy, (iii) psoriasis, (iv) rheumatoid arthritis, and (v) tumorigenesis [10]. Deciphering the mechanisms of normal and aberrant angiogenesis has assumed considerable therapeutic importance over the past 46 years owing to the initial studies of Folkman on tumorigenesis [11].

Angiogenesis is under stringent control and is regulated by both endogenous activators and inhibitors [6]. Four families of receptor protein-tyrosine kinases play pivotal roles in neovascularization. The VEGF/VEGFR family is the most studied regulator of vascular development and is the central focus of this review. The eph/Ephrin system controls positional guidance of the vasculature and arterio-venous asymmetry while the angiopoietin/Tie system controls vessel maturation and quiescence [12,13]. Fibroblast growth factors and their receptors also play important roles in neovascularization [14]. There are two co-receptors for the VEGF family: neuropilin-1 and neuropilin-2 [15]. The neuropilins contain an extracellular portion, a transmembrane segment, and a short (≈40 residues) intracellular domain that is devoid of enzymatic activity. Neuropilin-1 and neuropilin-2 can form complexes with each other and function in a cooperative fashion.

Angiostatin [16], endostatin [17], and thrombospondin [18] are endogenous anti-angiogenic factors. The action of these negative regulators predominates under most physiological conditions and angiogenesis is quiescent. Under various pathological conditions including tumor progression, the vasculature undergoes a so-called angiogenic switch where the action of positive regulators predominates and angiogenesis becomes active [19]. See Ref. [6] for a list of more than two dozen additional physiological pro-angiogenic and more than two dozen physiological anti-angiogenic factors. That such a large number of factors are at play indicates the complexity of the angiogenic process.

2.2. The VEGF family of growth factors

The important role of angiogenesis in the pathogenesis of renal cell carcinomas and other tumors has focused the attention of investigators on the biology of VEGFs and VEGFR1/2/3 and to the development of inhibitors of these intricate and multifaceted pathways. The physiological VEGF growth factors consist of the following: VEGF-A/B/C/D and placental growth factor (PlGF) [6]. These factors and their isoforms are encoded by the *VEGFA, VEGFB, VEGFC, VEGFD,* and *PGF* genes, respectively (Table 1). The active forms of these glycoproteins are homodimers that differ in their size and their ability to bind heparin, heparan sulfate, or to accessory transmembrane proteins called neuropilins, which limits their diffusibility and local activity.

The discovery of VEGF-A represented the convergence of experiments performed by several investigators in the 1980s. In 1983, Senger et al. characterized a protein from ascites fluid induced by a guinea pig hepatocellular carcinoma, which they assayed by its induction of vascular permeability [20]. In 1989, Ferrara and Henzel characterized a protein isolated from media conditioned by bovine pituitary folliculostellate cells, which they assayed by its vascular endothelial cell mitogenicity [21]. Connolly et al. purified vascular permeability factor (VPF) from media conditioned by a guinea pig hepatocellular carcinoma, which they assayed by its permeability enhancing activity; they found that this factor unexpectedly stimulated vascular endothelial cell proliferation [22]. These investigators prepared an antibody directed toward the amino-terminal 21 amino acids of VPF and showed that this antibody blocked both (i) vascular endothelial cell mitogenic and (ii) vascular permeability activities thereby providing strong evidence that a single entity possesses both activities, a surprising result at the time. Leung et al. reported the complete sequence of human VEGF-A as deduced from cDNAs isolated from human HL60 leukemia cells [23]. These independent analyses converged and demonstrated that the molecule with vascular endothelial mitogenic activity (VEGF) and that which enhances vascular permeability (VPF) are one and the same.

VEGF-A_{165} (the mature and processed form of which contains 165 amino acid residues) is the predominantly expressed isoform in humans followed by VEGF-A_{121} and VEGF-A_{189}. Muller et al. determined the X-ray crystal structure of human VEGF-A [24] and subsequent studies indicate that each of the other members of the VEGF family posses the same overall organization (VEGF-B, 2C7W; VEGF-C, 2X1W; VEGF-D, 2XV7; PlGF, 1FZV) [25–28]. VEGF-A consists of two identical antiparallel four-stranded β-sheet monomers linked by a disulfide bond from C51 of one monomer to C60 of the other monomer with a reciprocal disulfide bond from C60 of

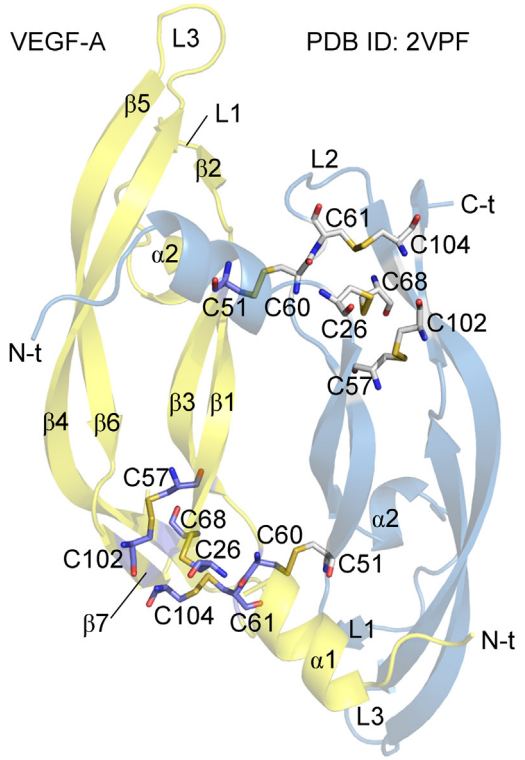

Fig. 1. Structure of the VEGF-A homodimer. N-t, N-terminus; C-t, C-terminus. Figs. 1, 3–6, 8 and 9 were prepared using the PyMOL Molecular Graphics System Version 1.5.0.4 Schrödinger, LLC.

the first monomer to C51 of the second (Fig. 1). Each monomer contains seven β-strands (β1-β7) along with two α-helices (α1 and α2). At the end of each monomer is a so-called cystine knot, which consists of two disulfide bonds forming a covalently linked ring between the contiguous β3- and β7-strands (C61–C104 and C57–C102) along with a third disulfide bond (C26–C68) passing through this ring and connecting the beginning of the β1- and β4-strands. Each VEGF-A monomer contains three loop regions that make contact with VEGFR2 as noted later. The loops connect the α2-β2 turn, the β3- and β4-strands, and the β5- and β6-strands (L1, L2, and L3 loops, respectively). The VEGF-A isoforms stimulate robust VEGFR2 autophosphorylation; they interact with VEGFR1, but the induction of its autophosphorylation is weak [29].

The next member of the VEGF family consists of two isoforms as a result of alternative pre mRNA splicing including VEGF-$B_{167/186}$ (Table 1) [6]. In adult mice, the greatest levels of VEGF-B mRNA occur in brain, heart, kidney and testes; lower levels occur in liver, lung, and spleen [30]. VEGF-B interacts with VEGFR1 and is implicated in fatty acid uptake in endothelial cells, most notably those in the heart [29]. VEGF-C is synthesized as a prepropeptide of 419 residues. It first forms an antiparallel homodimer linked by disulfide bonds. Before secretion, a cleavage occurs between Arg-227 and Ser-228 producing a heterotetramer. The next step of processing involves the enzyme-catalyzed hydrolytic removal of the N-terminal propeptide extracellularly as catalyzed by ADAMTS3 (a disintegrin and metalloprotease with thrombospondin type 1 motif 3) [31,32]. This process is aided by CCBE1 (collagen and calcium binding EGF domains 1). Mature VEGF-C is composed of two VEGF homology domains that include residues 112–227. VEGF-C activates VEGFR3 and participates in the genesis and maintenance of lymphatic vessels [6].

VEGF-D is synthesized and processed in a fashion similar to that of VEGF-C [6]. However, it does not undergo extracellular cleavage as catalyzed by ADAMTS3, but instead may be processed by plasmin [31,32]. The mature form consists of residues 89–205 and it activates VEGFR3 [29]. The unprocessed extracellular VEGF-C/D are able to activate VEGFR3, but not VEGFR2. However, proteolytic processing of these two factors enables them to activate VEGFR2 [33]. Human placental growth factor is synthesized as a 221-residue chain; following the cleavage of the signal peptide, the mature form contains residues 19–221. The glycoprotein forms a dimer similar to that of VEGF-A [6]. The factor is also expressed in nonplacental tissues. PlGF binds to VEGFR1, but its function appears to differ from that brought about by VEGF-A/B. VEGF-E is a nonhuman factor that is produced by the Orf parapoxvirus [34]. The factor supports the angiogenesis that accompanies parapoxvirus infections by stimulating VEGFR2. VEGF-F is another nonhuman factor that is found in some snake venoms [35].

2.3. The VEGF receptors

2.3.1. General properties

The VEGF receptor family consists of three protein-tyrosine kinases including VEGFR1 (Flt-1, fms-like tyrosyl kinase-1, where fms refers to feline McDonough sarcoma virus) [36], VEGFR2 (Flk-1/KDR, Fetal liver kinase-1/Kinase insert Domain-containing Receptor) [37], and VEGFR3 (Flt-4) [38,39]. Each of these receptors consists of an extracellular segment that contains seven immunoglobulin-like domains (IgDs), a transmembrane segment (TM), a juxtamembrane segment (JM), an intracellular protein-tyrosine kinase domain that contains a kinase insert domain (KID) of about 70 residues that occurs between the αD and αE helices, and a carboxyterminal tail (Fig. 2). Moreover, VEGFR3 undergoes a proteolytic cleavage in IgD6; the two components of the original chain remain linked by a disulfide bond. These enzymes, which are glycoproteins with a molecular weight of 180–220 kDa, catalyze the following reaction:

$$MgATP^{1-} + \text{protein-O} : H \rightarrow \text{protein-O} : PO_3^{2-} + MgADP + H^+$$

where —OH is the hydroxyl group found in the protein-tyrosine substrate. Note that the phosphoryl group (PO_3^{2-}) and not phosphate group (OPO_3^{2-}) is transferred from ATP to the substrate protein.

The VEGF receptors (type V) are related to the macrophage colony stimulating factor-1 receptor, the platelet-derived growth factor receptors-α/β, and Kit (type III), and the fibroblast growth factor receptors1/2/3/4 (type IV), each of which contains extracellular immunoglobulin-like domains and a kinase insert. See Ref. [40] for a description of the type I–IX protein-tyrosine kinase receptors. In adults, VEGFR1 and VEGFR2 are found chiefly in vascular endothelial cells while VEGFR3 is localized in lymphatic endothelial cells [19]. The major functions of these receptors and their ligands are listed in Table 2. With increases in sensitivity, these receptors have been found in numerous other cell types, tissues, and organs [29]. For example, VEGF1 is found in monocytes, macrophages, vascular smooth muscle cells, and neuronal cells. Moreover, VEGFR3 is expressed in neural progenitors, macrophages, and osteoblasts. VEGF-A, VEGF-C, VEGFR1 [41], VEGFR2 [42], and VEGFR3 [43] null mice are embryonic lethal. The deficient expression of each of these gene products is associated with the improper development of the circulatory system. However, nonexpression of VEGF-B, VEGF-D, and PlGF in mice is compatible with life.

Besides the transmembrane receptor form, alternative splicing of VEGFR1 pre-mRNA produces a soluble VEGFR1 receptor isoform (sVEGFR1) that can bind to and thereby inhibit the action of VEGF-A [44]. After the signal peptide is removed sVEGFR1 contains the 661 amino acid residues corresponding to the first six of seven immunoglobulin-like domains. sVEGFR1 that is produced by the human placenta and released into the circulation

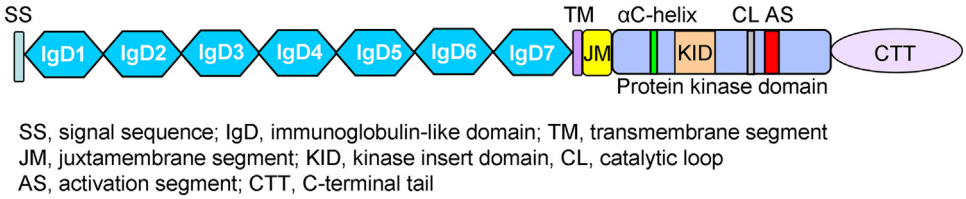

Fig. 2. Overall structure of VEGFR1/2/3.

Table 2
VEGF receptors, ligands, and functions.[a]

Receptor	VEGFR1	VEGFR2	VEGFR3
Ligands	VEGF-A[b], VEGF-B[b], PlGF[b]	VEGF-A[b], VEGF-C[c], VEGF-D[c], VEGF-E[d], VEGF-F[e]	VEGF-C, VEGF-D
Functions	Vasculogenesis and monocyte/macrophage motility; a negative regulator of angiogenesis	Vasculogenesis, angiogenesis, vascular permeability, and endothelial cell motility and survival	Vascular and lymphatic development and maintenance

[a] Data from Ref. [6,29].
[b] Multiple isoforms produced by alternative pre-mRNA splicing.
[c] Ligand must be proteolytically processed.
[d] Non-human factor encoded by the Orf parapoxvirus.
[e] Non-human factor found in some snake venoms.

of the mother produces the hypertension and proteinuria characteristic of pre-ecclampsia [45,46]. Although PlGF is unable to stimulate endothelial cell proliferation, it may potentiate proliferation of these cells with suboptimal VEGF-A concentrations. This potentiation by PlGF may contribute to angiogenesis during tumor progression. Park et al. hypothesized that VEGFR1 binds to and inhibits VEGF-A action, acting as a decoy by preventing VEGF-A binding to VEGFR2 [47]. Thus, sVEGFR1 appears to control the activity of VEGFR2 by modulating the availability of VEGF-A. Ebos et al. found a soluble truncated form of VEGFR2 (sVEGFR2) in the circulation of humans and mice [48]. The level of circulating sVEGFR2 has been considered as a potential biomarker of VEGF-dependent tumor growth [49], but the role of this alternatively spliced variant remains unclear.

Leppänen et al. determined the X-ray crystal structure of VEGF-C bound to VEGFR2 and found that IgD2 and IgD3 of the receptor make up the high-affinity binding site [26]. Based upon alanine scanning mutagenesis experiments, Jeltsch et al. found that VEGF-C binding to VEGFR3 requires IgD1 and IgD2 [50]. In contrast, Leppänen et al. prepared VEGFR1/VEGFR2 chimeras and reported that the binding of VEGF-A to VEGFR1 involves predominately IgD2 [26]. They found that the VEGF-C dimer interacts with two VEGFR2 molecules. As a result of VEGF-induced VEGFR2 dimer activation, one receptor protein kinase domain is able to catalyze the phosphorylation and activation of the other protein kinase by the *trans*-autophosphorylation of two tyrosine residues within the activation segment. In the case of VEGFR2, the phosphorylation of activation segment tyrosines is preceded by the *cis*-autophosphorylation of Y951 within the kinase insert [51]. The newly activated protein kinase is then able to catalyze the phosphorylation of two tyrosine residues within the activation segment of the first enzyme resulting in enzyme activation [52,53].

Sarabipour et al. characterized the interactions between human VEGFR2 monomers that were labeled with the yellow fluorescent protein (YFP) or mCherry (a fluorescence resonance energy transfer (FRET) donor-acceptor pair) in plasma membrane-derived vesicles generated from transfected Chinese hamster ovary cells [54]. They found that VEGFR2 dimers form when expressed at physiological levels. Furthermore, they reported that VEGF-A binding led to a conformational change in the transmembrane segment and this was accompanied by phosphorylation in the protein kinase domain. Such phosphorylation was stimulated by VEGF-$A_{121/165}$ and VEGF-C/D/E. They found that inter-receptor contacts within the extracellular and transmembrane domains are important for the formation of the unliganded dimer and for the transition to the VEGF-A induced active conformation. These investigators found that IgD4 and IgD7 were important both for the formation of unliganded and liganded VEGFR2 dimers. They also demonstrated that the C482R $VEGFR2_{IgD5}$ mutation, which is linked to infantile hemangiomas, promotes ligand-independent signaling by mimicking the structure of the ligand-bound wild-type VEGFR2 dimer. Ligand-independent dimer formation has also been reported for other receptor protein-tyrosine kinases including EGFR, FGFR, and Trk.

Autophosphorylation of tyrosines in the activation loop within the kinase domain results in stimulation of enzyme activity and the *trans*-autophosphorylation of tyrosines in the other regions generates docking sites for modular domains that recognize phosphotyrosine in sequence-specific contexts [55]. Kendall et al. prepared single and double Y1054F and Y1059F mutants of VEGFR2 [53]. They reported that partial activation of VEGFR2 occurs following the phosphorylation of Tyr1054 or Tyr1059. However, full activation requires the phosphorylation of both residues. The insulin receptor protein-tyrosine kinase is activated by the phosphorylation of three tyrosine residues within the activation segment and the obligatory order of phosphorylation is Y1162 followed by that of Y1158 and then Y1163 [56]. Whether the phosphorylation of Y1054 and Y1059 occurs in a random fashion or is ordered was not pursued by Kendall et al. [53].

In contrast to VEGFR2, Kendall et al. reported that VEGFR1 fails to undergo significant activation segment phosphorylation and activation [53]. As noted later, VEGFR1 contains all of the signature sequences of a kinase-active enzyme. To explain its impaired activity, Meyer et al. noted that its activation segment contains an Asn1050 while VEGFR2/3, PDGFRα/β, CSF-1R, Kit, and Flk-2 contain an aspartate at the equivalent position [57]. They prepared chimeric constructs with the extracellular domain of CSF-1R fused to wild type and mutant VEGFR1 and VEGFR2. They found that an N1050D mutation in VEGFR1 displayed increased autophosphorylation and enzyme activation while the reverse mutation in VEGFR2 resulted in decreased autophosphorylation. In examining the X-ray crystal structures of the catalytic domains of VEGFR1 (PDB ID: 3HNG) and

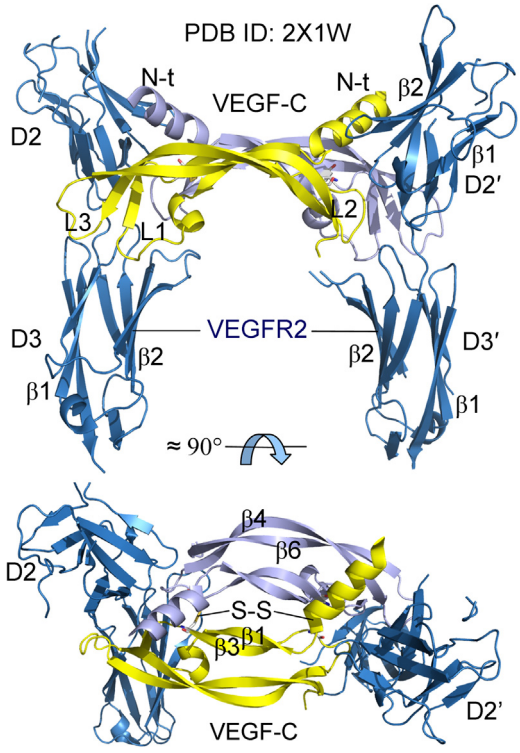

Fig. 3. Structure of the VEGF-C homodimer bound to the IgD2/3 and IgD′2/3 domains of VEGFR2. N-t, N-terminus of VEGF-C; S-S disulfide bonds linking the two VEGF-C monomers together (the disulfide bridge on the right is hidden in this view).

VEGFR2 (PDB ID: 4ASD), the reason for the differences in the activity of the activation segment mutants is not readily apparent. Like VEGFR2, Salameh et al. demonstrated that VEGFR3 undergoes activation segment phosphorylation at residues 1063 and 1068 [58]. However, mutation of activation segment Y1063 showed only a minor reduction of the receptor phosphorylation when compared with the wild type protein. This finding demonstrates that Y1068 phosphorylation, but not Y1063 phosphorylation, is required for VEGFR3 activation.

Leppänen et al. found that the L1 and L3 loops of one component of the VEGF-C dimer binds to IgD2 and IgD3 of one VEGFR2 while the L2 loop binds to the IgD2′ domain of a second VEGFR2; there is a reciprocal interaction where the L1 and L3 loops of the second component of the VEGF-C dimer binds to IgD2′ and IgD3′ of the second VEGFR2 monomer while its L2 loop binds to IgD2 of the first VEGFR2 (Fig. 3A) [26]. They found that both IgD2 and IgD3 consist of two β-sheets (β1 and β2). Both the IgD2 and IgD3 domains contain a disulfide bridge within a hydrophobic core (not shown). The IgD2 and IgD3 domains of each VEGFR2 are orthogonal to VEGF-C. The structure of VEGF-C is that of an antiparallel homodimer that is covalently linked together by two disulfide bridges (Fig. 3B) as described above for VEGF-A.

2.3.2. Structures of the VEGFR1/2/3 and FGFR protein kinase domains and the K/E/D/D motif

The classical protein kinase catalytic domains consist of about 250–300 amino acid residues. However, VEGFR1/2/3 protein kinase domains contain inserts of about 70 residues yielding overall lengths that consist of about 330 amino acids [59]. The determination of the tertiary structure of the catalytic subunit of PKA bound to a polypeptide antagonist by Knighton et al. has illuminated many of the fundamental properties of this enzyme superfamily (PDB ID: 2CPK) [60,61]. All protein kinases have a small N-terminal lobe and large C-terminal lobe (Fig. 4A) [62]. The small lobe contains five β-strands (β1–5) along with a regulatory αC-helix; the large lobe is mostly helical (it contains seven helices: αD–αI and αEF) along with four short β-strands (β6–β9). A gap or cleft between the N-terminal and C-terminal lobes interacts with the ATP nucleotide substrate. Of the hundreds of known protein kinase structures, all of them exhibit the traditional protein kinase fold described first for the PKA catalytic subunit [60,61]. Because of the unavailability of a structure of an active VEGFR protein kinase domain with a visualizable activation segment, FGFR2 was chosen for comparative purposes. This receptor-enzyme, which is related to the VEGFR family, contains three immunoglobulin-like extracellular domains and a short kinase insert of about 15 amino acid residues [40,59].

Hanks and Hunter analyzed the sequences of several dozen protein kinases and they divided the primary structures into 12 portions (I-VIA,VIB-XI) [63]. Like all protein kinases, Domain I of the VEGFR family contains the Gly-rich loop (GRL) with a GxGxΦG signature where Φ is usually a hydrophobic residue; in the case of the VEGFR family, Φ is phenylalanine (Table 3). This loop connects the β1- and β2-strands and sits over the ATP-binding site (Fig. 4A). The Gly-rich loop of protein kinases is quite flexible as required by the conformational changes necessary for ATP binding and ADP release during each catalytic cycle. Domain II of VEGFR2 contains a conserved Ala-Xxx-Lys (^{866}AVK^{868}) sequence in the β3-strand and domain III contains a conserved glutamate residue (E885) within the αC-helix that forms an electrostatic bond with the conserved AVK-lysine. Domain VIB of VEGFR1/2/3 contains an evolutionarily conserved HRD sequence, which forms part of the catalytic loop (HRDLAARN) that begins with histidine and ends with an asparagine. Domain VII of the VEGFR family contains the classical DFG signature and domain VIII, an APE sequence; together these residues represent the beginning and end of the protein kinase activation segment. For VEGFR1/2/3 and FGFR2 the activation segment consists of 30 amino acid residues and the distance from its beginning to end is about 21 Å. Domains IX–XI contain the conserved αF–αI helices. These 12 domains were described prior to the knowledge of the tertiary structure of any protein kinase and the elucidation of the structure of the catalytic subunit of protein kinase A provided an invaluable framework for understanding their roles in catalysis.

Nearly all active protein kinases contain a K/E/D/D (Lys/Glu/Asp/Asp) signature that plays an indispensable role in the protein kinase catalytic cycle (Table 3) [64]. In contrast, so-called pseudokinases (which may have minimal activity or none at all) lack this tetrad. For example, inactive ErbB3/HER3 within the EGFR family contains the signature sequence K/E/N/D where the catalytic aspartate is replaced by an asparagine [65]. For investigators who want to prepare a kinase-dead enzyme, this can be accomplished by mutating the K/E/D/D lysine to methionine. The first two residues function together within the N-terminal lobe and the two aspartate residues function within the C-terminal lobe. Although both lobes contribute to ATP binding, the amino-terminal lobe plays a more important role in this process. Based upon the structures of other enzymes, we deduce that the K of K/E/D/D from the β3-strand of VEGFR1/2/3 holds the α- and β-phosphates of ATP in an active position. The carboxylate group of the αC-helix E of K/E/D/D forms an electrostatic bond with the ε-amino group of the β-strand lysine and the latter also interacts with the α- and β-phosphates. The existence of an electrostatic bond between the β3-lysine and αC-glutamate is required for the formation of an active protein kinase structure; such a structure is called the αC_{in} configuration as depicted in Fig. 4A–C. When the lysine and glutamate residues fail to make contact, such an inactive structure is called the αC_{out} configuration (see Ref. [64] for details). For the entire protein kinase enzyme family, the αC_{in} configuration is necessary, but not sufficient, for catalytic activity.

Table 3
Composition and important residues of the human VEGF receptors.

	VEGFR1	VEGFR2	VEGFR3	Inferred function	Hanks no.
Signal sequence	1–26	1–19	1–24		
Extracellular domain	27–758	20–764	25–775		
IgD1	32–123	46–110	30–127	Increases VEGF binding affinity (VEGFR1 only)	
IgD2	151–214	141–207	151–213	Binds VEGFs	
IgD3	230–327	224–320	219–326	Binds VEGFs	
IgD4	335–421	328–414	331–415	Makes mirror-image homotypic contacts with a sister receptor and increases ligand binding	
IgD5	428–553	421–548	422–552	See IgD4	
IgD6	556–654	551–660	555–617	Increases ligand binding	
IgD7	61–747	667–753	678–764	See IgD4	
Transmembrane segment	759–780	765–789	776–797	Links extracellular and intracellular domains and mediates dimer formation	
JM segment	781–826	790–833	798–844	Regulatory role	
Protein kinase domain	827–1158	834–1162	845–1173	Catalyzes transphosphorylation	
Glycine-rich loop	GRGAFG, 834–839	GRGAFG, 841–846	GYGAFG, 852–857	Anchors ATP β-phosphate	I
KID	827–1158	834–1162	845–1173	Contains a signal transduction autophosphorylation site in VEGFR2	None
β3-K of K/E/D/D	861	868	879	Forms salt bridges with ATP α- and β-phosphates and with β3-K	II
αC-E, E of K/E/D/D	878	885	896	Forms salt bridges with β3-K	III
Hinge residues				Connects N- and C-lobes	V
Catalytic loop, HRDLAARN	1019–1027	1026–1033	1035–1042	Plays both structural and catalytic functions	VIb
Catalytic loop HRD, First D of K/E/D/D	1022	1028	1037	Catalytic base (abstracts protein substrate proton)	VIb
Catalytic loop Asn, HRDLAARN	1027	1033	1042	Chelates Mg^{2+}(2)	VIb
AS DFG, Second D of K/E/D/D	1040–1042	1046–1048	1055–1057	Chelates Mg^{2+}(1)	VII
AS	1040–1069	1046–1075	1055–1084	Positions protein substrate	VII–VIII
AS tyrosines	1048[a], 1053[a]	1054, 1059	1063, 1068	Stabilizes the AS after phosphorylation	VIII
APE	1067–1069	1073–1075	1082–1084	Interacts with the αHI loop and stabilizes the AS	VIII
C-terminal tail	1159–1338	1163–1356	1174–1298	Inhibitory domain	None
C-terminal tail tyrosine phosphorylation sites	1169, 1213,1242,1309, 1327, 1333	1175, 1214, 1223, 1305, 1309, 1319	1230, 1231, 1265, 1333, 1337, 1363	Phosphorylated tyrosines interact with a variety of docking proteins that mediate intracellular signaling	None
No. of residues	1338	1356	1298/1363		
Molecular Wt[b] (kDa)	150,769	151,527	145,599/152,757		
Swiss-Prot accession no.	P17948	P35968	P35916		

[a] Not phosphorylated.
[b] Molecular weight of the unprocessed and nonglycosylated precursor.

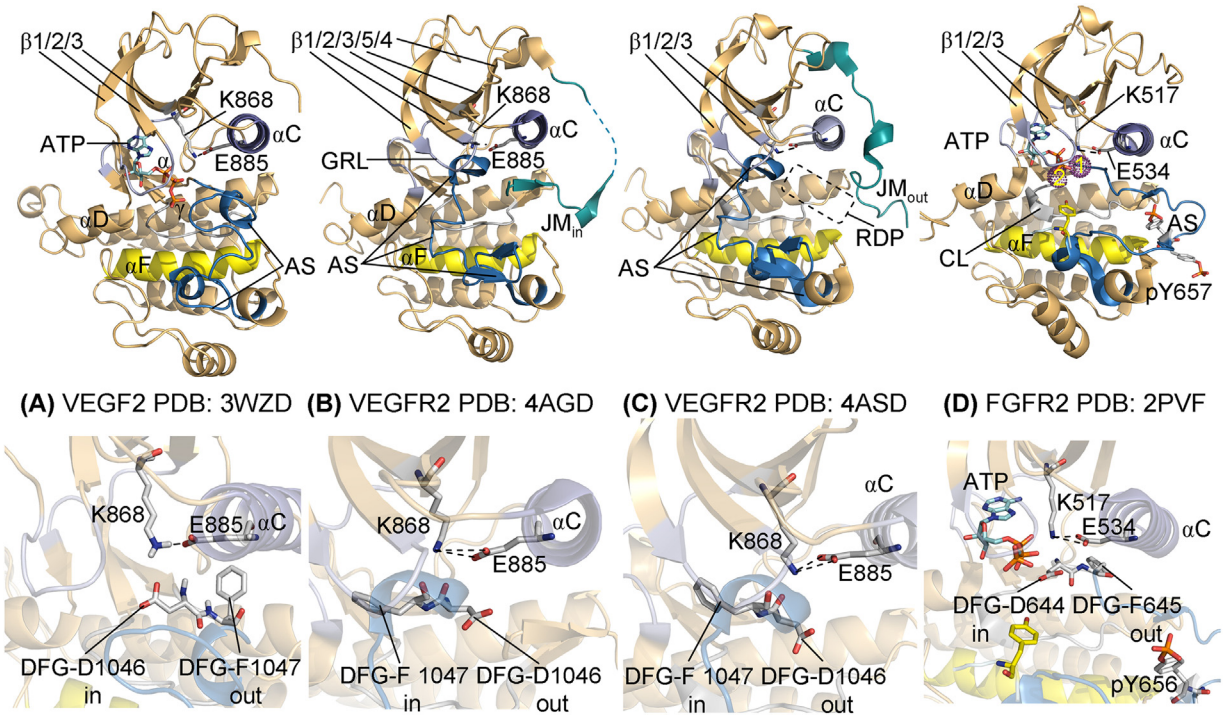

Fig. 4. (A) Inactive VEGFR2 with a compact activation segment and the DFG-D_{in} configuration. (B) Inactive VEGFR2 with a compact activation segment and the DFG-D_{out} and JM_{in} configuration. (C) Inactive VEGFR2 with a compact activation segment and the DFG-D_{out} and JM_{out} configuration. (D) Active FGFR2 with an open activation segment and the DFG-D_{in} configuration. The dashed lines in the lower figures represent polar bonds. AS, activation segment; CL, catalytic loop; GRL, Gly-rich loop; JM, juxtamembrane segment; RDP, regulatory domain pocket.

The carboxyterminal lobe is responsible for protein substrate binding.

Two Mg^{2+} ions participate in the catalytic cycle of a several protein kinases [32,66] and are most likely required for the functioning of the VEGF receptors. By inference, the DFG-D binds to $Mg^{2+}(1)$, which in turn binds to the β- and γ-phosphates of ATP. In the active enzyme form, DFG-D points inward toward the active site. In the less active form of many protein kinases, including that for VEGFR2 as shown in Fig. 4B, DFG-D is directed outward from the active site (protein kinase inhibitors that bind to the DFG-D outward conformation are classified as type II inhibitors [67]). The asparagine of the catalytic loop (HRDLAARN) binds $Mg^{2+}(2)$, which in turn interacts electrostatically with the α- and γ-phosphates of ATP. HRD-D1028 of VEGFR2 functions as a base and accepts a proton from the protein-tyrosyl residue group during catalysis (Fig. 5).

We infer that the activation segment of the VEGFR active conformation forms an open structure that promotes protein binding; such an open structure is depicted for FGFR2 (Fig. 4D). In the dormant enzyme, the activation segment forms a compact and closed structure that disallows protein substrate binding (Fig. 4A and B). The 6-amino group of ATP typically functions as a hydrogen bond donor with the carbonyl backbone of the first protein kinase hinge residue that connects the amino-terminal and carboxyterminal lobes while the *N*1 nitrogen of adenine forms a second hydrogen bond with the N—H group of the third hinge residue (not shown).

2.3.3. Function of the juxtamembrane segment

McTigue et al. compared the binding properties and X-ray structures of several drugs with VEGF2 with and without the juxtamembrane (JM) segment [68]. The binding of several drugs including axitinib, pazopanib, sunitinib, and sorafenib to VEGFR2 containing the JM segment parallels their efficacy in inhibiting VEGFR2 in cells in culture in contrast to VEGFR2 lacking the JM segment. They reported that VGFR2 exhibits two conformations of the JM segment: JM_{in} and JM_{out}. Several residues from JM_{in} (820–826) are found over the αC-helix. Moreover, the JM_{in} conformation folds into the interdomain space adjacent to the αC-helix (Fig. 4B) within the so-called regulatory domain pocket, or RDP. This is the space where DFG resides in active enzymes and it is not possible for VEGFR2 to assume the DFG-D_{in} state in enzymes with JM_{in}. The displacement of the JM segment from the regulatory domain pocket yields a JM_{out} conformation (Fig. 4C).

The JM segment of VEGFR2 and VEGFR3, but not that of VEGFR1, contains protein-tyrosine phosphorylation sites [51,69]. Solowiej et al. examined the mechanism of VEGFR2 JM segment Y801 autophosphorylation using purified protein [51]. They found that its rate of phosphorylation did not vary with protein concentration and this result is compatible with an intramolecular *cis*-autophosphorylation reaction. These investigators pointed out that such intramolecular autophosphorylation reactions are rare, but not without precedent. Gavagni et al. studied the phosphorylation of human VEGFR3 in cultured cells that is initiated by cellular attachment to the extracellular matrix [69]. They identified the sites of phosphorylation as Y830/833/853 within the JM segment, Y1063 within the kinase insert, and Y1333/1337 in the carboxyterminal tail. They found that these VEGFR3 sites were phosphorylated using kinase-dead VEGFR3 and they demonstrated that recombinant Src catalyzed VEGFR3 phosphorylation in detergent-extracted human umbilical vein endothelial cells (HUVECs). These experiments indicate that Src participates in VEGFR3 signaling.

2.3.4. Function of the kinase insert domain and carboxyterminal tail in signaling

Manni et al. examined the role of the kinase insert domain and the carboxyterminal tail in the regulation of VEGFR2 activity by preparing deletion mutants [70]. They found that protein kinase domain constructs lacking either of these domains had increased enzyme activity as determined by measuring the phosphorylation

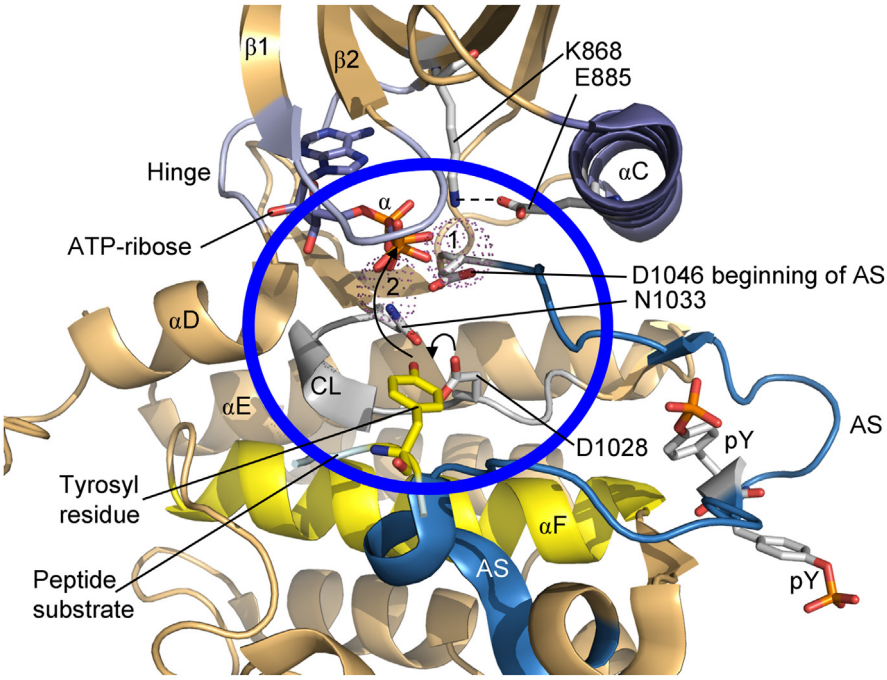

Fig. 5. Inferred mechanism of the VEGFR2 protein kinase reaction. The chemistry occurs within the blue circle. The dotted spheres represent $Mg^{2+}(1)$ and $Mg^{2+}(2)$. PDB ID: 1PKG (FGFR2) was used as a template, but the residue numbers correspond to VEGFR2. AS, activation segment; CL, catalytic loop; pY, phosphotyrosine.

of Y1054 and Y1059 within the activation loop. This indicates that these two domains are inhibitory. Paradoxically, deletion of both the kinase insert and the carboxyterminal tail gave rise to diminished enzyme activity. Moreover, these investigators found that these two domains promote enzyme dimerization. They examined the order of phosphorylation of the various tyrosine residues within VEGFR2. They find that phosphorylation of Y801 within the juxtamembrane segment occurs initially and this is hypothesized to relieve JM_{in} inhibition. This phosphorylation is followed by activation loop phosphorylation at residues Y1054/1059. Then phosphorylation of Y1214 within the carboxyterminal tail occurs before the phosphorylation of Y951 within the insert domain and then Y1175 within the tail. They found that phosphorylation of Y1175 in the carboxyterminal tail was severely reduced in the insert domain-deleted mutants. pY1175 serves as a docking site for phospholipase Cγ1, an important downstream signaling protein. Thus, the carboxyterminal tail functions in an inhibitory fashion while phosphorylation of the kinase insert facilitates Y1175 phosphorylation and downstream signaling. In contrast to VEGFR2/3, VEGFR1 is not phosphorylated within the kinase insert so that its signaling pathways are regulated differently [70].

Simons et al. reported that phosphorylation of pY1173 in mice (equivalent to pY1175 in humans) binds to and activates PLCγ1 resulting in the generation of the inositol 1,4,5-trisphosphate second messenger and the consequent release of Ca^{2+} from intracellular stores [29]. This leads to the activation of protein kinase C-β2 and activation of the Raf-MEK-ERK1/2 signaling module. This pathway participates in cell growth, proliferation, migration, and survival [71]. Activation of VEGFR2 also leads to the activation of the Src protein kinase, which is dependent upon mouse pY949 (human pY951). This residue, which is an autophosphorylation site within the kinase insert domain, binds to T cell-specific adapter (TSAd) leading to Src activation by mechanisms that are unclear [29]. Src participates in the activation of the phosphatidyl inositol 3-kinase/AKT pathway involved in cell survival [66]. Other signaling modules activated by VEGFR2 include (i) stress-activated protein kinase-2 (p38 MAP kinase) by a mechanism that is unclear and (ii) signal transducers and activators of transcription (STAT1/6) that apparently results from direct phosphorylation by VEGFR2 and not by Janus kinase 1 (JAK1) [29].

VEGF-A binds to VEGFR1 with higher affinity than it binds to VEGFR2 (≈10 pM vs. 75–750 pM) [6]. Both VEGFR1 and sVEGFR1 are thought to modulate the concentrations of VEGF-A and control the stimulation of VEGFR2. In contrast to VEGFR2, VEGFR1 has weak tyrosine kinase phosphorylation activity following stimulation by the VEGF ligands. Phosphorylation sites have been reported in the juxtamembrane domain, the activation segment, and the carboxyterminal tail, but downstream signaling pathways have not been determined. VEGFR1 is expressed in monocytes and macrophages where it plays a role in cell migration. VEGF-B has been implicated in fatty acid uptake in endothelial cells by increasing the expression of fatty acid transport proteins (FATPs) including FATP-1 and FATP-4 [72]. This process is mediated by VEGFR1 [73].

VEGFR3 participates in lymphangiogenesis [6]. VEGFR3, but not VEGFR2, binds to unprocessed VEGF-C and VEGF-D. Proteolytically processed VEGF-C and VEGF-D bind with high affinity to both VEGFR2/3. Moreover, these processed ligands appear to promote the formation of VEGFR2-VEGFR3 heterodimers. Heterodimers of VEGFR1-VEGFR2 have also been described [74,75], but the biological role of both sets of heterodimers has not been elucidated. Phosphorylation sites have been identified in the activation segment and carboxyterminal tail (Table 3), but their precise role in signal transduction has not been clarified. However, activation of VEGFR3 leads to the activation of ERK1/2 and to AKT signaling [29]. For comprehensive reviews on VEGF family signaling see Refs. [29,33,75].

2.3.5. *Hydrophobic spines in active and dormant protein kinases*

Kornev et al. analyzed the structures of the active and dormant conformations of about two dozen protein kinases by a local spatial pattern alignment algorithm [76,77]. They found that this algorithm grouped four hydrophobic residues together to produce a so-called regulatory or R-spine [76] and it grouped eight hydrophobic residues together to produce a catalytic or C-spine (Fig. 6A)

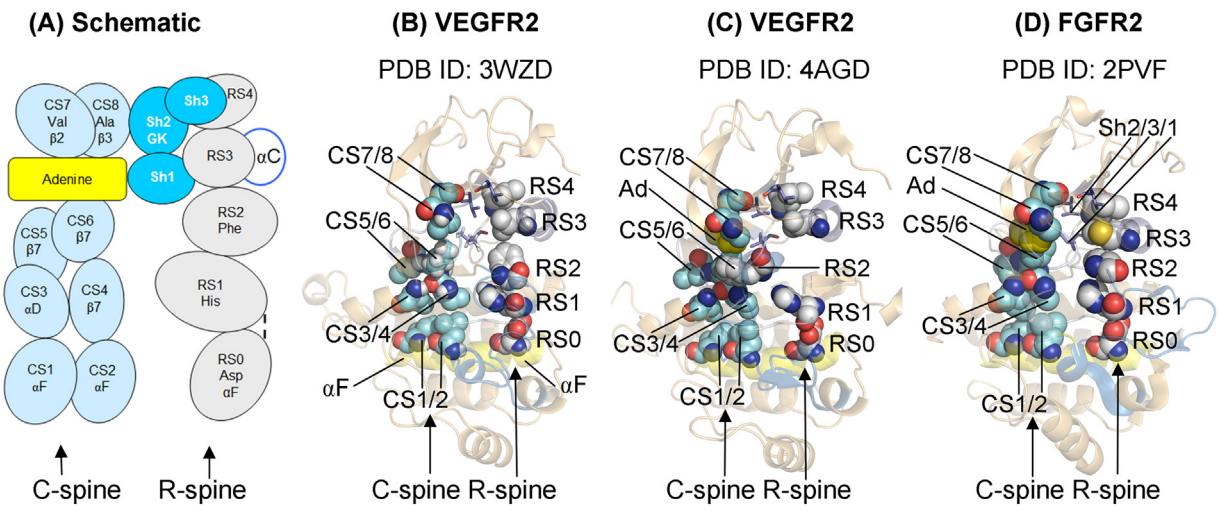

Fig. 6. (A) Schematic view of the spine and shell residues. (B) Spines of an inactive DFG-D_{in} VEGFR2 showing an upward displacement of RS3/4 with respect to RS2. The C-spine adenine has been omitted. (C) Spines of an inactive DFG-D_{out} VEGFR2 showing a broken R-spine with the leftward displacement of RS2. (D) Linear spines of active FGFR2. Ad, adenine.

[77]. Each of these spines consists of amino acids found in both the small and large lobes. The R-spine contains one residue from the activation segment and another from the αC-helix; both of these components are key regulatory elements that determine high activity and low activity states. The C-spine contains the adenine base of ATP as one of its components. The R-spine serves as an anchor for the catalytic residues and stabilizes the interaction of the αC-helix, the activation segment, and the catalytic loop while the C-spine binds ATP within the cleft between the small and large lobes thus enabling catalysis. Moreover, Kornev et al. [77] concluded that the accurate alignment of both spines is required for the formation of an active enzyme as described for ALK, EGFR, ERK1/2, the cyclin-dependent protein kinases, the Janus kinases, and MEK1/2 as well as Src [7,64–67,71,78–81].

The R-spine contains a residue at the beginning of the β4-strand of the small lobe, a residue near the carboxyterminal end of the αC-helix (it is four residues distal to the conserved αC-glutamate), the DFG-Phe, and the HRD-His [76]. The N—H group of the HRD-His is anchored to the hydrophobic αF-helix within the large lobe by a hydrogen bond to an invariant aspartate carboxylate group. Meharena et al. labeled the R-spine residues as RS0, RS1, RS2, RS3, and RS4 [82]. The RS3/4 residues of a dormant form of VEGFR2 are tilted upward and away from RS2 (Fig. 6B). The DFG-D_{out} form of dormant VEGFR2 is displaced laterally while the R-spine of active enzymes including FGFR2 is linear (Fig. 6C–D).

The two residues of the small lobe of protein kinases that interact with the adenine base of ATP include a conserved valine near the beginning of the β2-strand (CS7) and a conserved alanine from the invariant AxK of the β3-strand (CS8). Moreover, a β7-strand hydrophobic residue (CS6) interacts with adenine. The CS6 residue is flanked by two residues labeled CS4 and CS5 that make hydrophobic contact with the CS3 residue near the beginning of the αD-helix. These three residues (CS5/6/4) occur immediately after the asparagine residue of the catalytic loop (HRDLAARN). Finally, CS3 and CS4 interact with CS1 and CS2 within the αF-helix to complete the catalytic spine [77]. Note that the hydrophobic αF-helix anchors both the catalytic and regulatory spines (Fig. 6). Furthermore, both spines play an important role in supporting the protein kinase catalytic residues in an active state. When comparing the spatial locations of the spinal residues, the greatest divergence in the structures between active and dormant protein kinases usually involves RS2 and RS3.

Using site-directed mutagenesis, Meharena et al. identified three residues within the catalytic subunit of PKA that stabilize the regulatory spine; they named these residues Sh1, Sh2, and Sh3, where Sh refers to shell [82]. The Sh2 residue is the so-called gatekeeper. This term signifies the role that this amino acid plays in permitting access to a back pocket [83,84], or back cleft; this portion of the enzyme occurs between the gatekeeper and the αC-helix. Small residues such as glycine, alanine, serine, cysteine, threonine, and valine permit the extension of drugs into the back pocket while medium sized residues such as isoleucine, leucine, methionine and glutamine are more restrictive [85]. Large residues such as phenylalanine and tyrosine are the most restrictive and disallow extension of drugs into the back pocket. The amino acids that constitute the R- and C-spines were identified by their location in active and dormant protein kinases based upon their three-dimensional X-ray crystallographic structures [76,77]. This is in contrast to the identification of the DFG or HRD signatures, which was based upon their canonical amino acid sequences [63]. Table 4 provides a listing of the spine and shell residues of human VEGFR1/2/3, FGFR2, and murine PKA. Nearly all ATP-competitive small molecule protein kinase inhibitors interact with residues that make up the C-spine and sometimes the Sh1 residue within the αC-β4 loop [67].

As we will see in the next section, many VEGFR2 inhibitors make hydrophobic contact with CS6/7/8, Sh1/2, and DFG-F (RS2). In several instances the antagonists form polar bonds with one or two residues within the hinge, the αC-glutamate, the β3-lysine, and DFG-D1046.

3. Pharmacological treatment of metastatic renal cell carcinomas

3.1. Structure of VEGFR2-drug complexes

Axitinib is an inhibitor of VEGFR1/2/3 protein-tyrosine kinases that is approved as a second-line treatment for metastatic renal cell carcinomas (Table 5). The X-ray structure shows that the N—H group of the axitinib indazole scaffold (Fig. 7A) forms a hydrogen bond with the hinge E917 carbonyl group of VEGFR2 while the *N*2 nitrogen of the scaffold forms a second hydrogen bond with the N—H group of the F918 [68]. Because the enzyme has the DFG-D_{out} conformation, the αC-E885 carboxylate is able to form a hydrogen bond with the benzamide N—H group while the DFG-D1046 N—H group forms a hydrogen bond with the benzamide carbonyl

Table 4
Spine and shell residues of human VEGFR1/2/3, FGFR2, and murine PKA.

	Symbol	KLIFS No.[a]	VEGFR1	VEGFR2	VEGFR3	FGFR2	PKA[b]
Regulatory spine							
β4-strand (N-lobe)	RS4	38	L894	L901	L912	L550	L106
C-helix (N-lobe)	RS3	28	L822	L889	L900	M538	L95
Activation loop F of DFG (C-lobe)	RS2	82	F1041	F1047	F1055	F654	F185
Catalytic loop His/Tyr (C-lobe)	RS1	68	H1020	H1026	H1035	H624	Y164
F-helix (C-lobe)	RS0	None	D1081	D1087	D1096	D685	D220
R-shell							
Two residues upstream from the gatekeeper	Sh3	43	V907	V914	V925	V562	M118
Gatekeeper, end of β5-strand	Sh2	45	V909	V916	V927	V564	M120
αC-β4 loop	Sh1	36	V892	V899	V910	I548	V104
Catalytic spine							
β3-AxK motif (N-lobe)	CS8	15	A859	A666	A977	A515	A70
β2-strand (N-lobe)	CS7	11	V841	V848	V859	V495	V57
β7-strand (C-lobe)	CS6	77	L1029	L1035	L1044	L633	L173
β7-strand (C-lobe)	CS5	78	L1030	L1036	L1045	V634	I174
β7-strand (C-lobe)	CS4	76	I1028	I1034	I1043	V632	L172
D-helix (C-lobe)	CS3	53	L917	L924	L935	L572	M128
F-helix (C-lobe)	CS2	None	L1088	L1094	L1103	L692	L227
F-helix (C-lobe)	CS1	None	I1092	I1098	I1007	I696	M231

[a] Ref. [83].
[b] From Refs. [76,77,82].

Table 5
Properties of FDA-approved orally effective small molecule VEGFR inhibitors.

Name, code, trade name®	Targets	PubChem CID	Formula	MW (Da)	VEGFR2 K_i (nM)[a]	D/A[b]	cLogP[c]	Inhibitor type[d]	FDA-approved indications[e] (year)[f]
Axitinib, AG-013736, Inlyta	VEGFR1/2/3, PDGFRβ, Kit	6450551	$C_{22}H_{18}N_4OS$	386.5	0.25	2/4	4.2	IIA	RCC (2012) after failure of one therapy
Cabozantinib, XL-184 and BMS-907351, Cometriq	VEGFR1/2/3, MET, Kit, Flt-3, Tie-2, TrkB, Axl	25102847	$C_{28}H_{24}FN_3O_5$	501.5	7	2/7	5.4	IIA	Medullary thyroid cancer (2012); RCC (2016) after one prior anti-angiogenic therapy
Lenvatinib, E7080, Lenvima	VEGFR2, FGFR1/2/3/4, PDGFRα, Kit, Ret	9823820	$C_{21}H_{19}ClN_4O_4$	426.9	4 (5 R3)	3/5	2.8	I½A	Thyroid cancer (2015); RCC (2016) in combination with everolimus after one anti-angiogenic therapy
Sorafenib, BAY 43-9006, Nexavar	VEGFR2, PDGFRβ, Raf	216239	$C_{21}H_{16}ClF_3N_4O_3$	464.8	0.002–0.1	3/7	4.1	IIA	RCC (2005); HCC (2007); Thyroid cancer (2013)
Sunitinib	VEGFR2, PDGFRβ, Kit	5329102	$C_{22}H_{27}FN_4O_2$	398.5	1.5	3/4	2.6	IIB	RCC (2006); GIST (2006), pancreatic neuroendocrine tumors (2011)
Pazopanib, GW786034, Votrient	VEGFR1/2/3, Kit, PDGFR	10113978	$C_{21}H_{23}N_7O_2S$	437.5	8–14	2/8	3.1	IIA[g]	RCC (2009); advanced soft tissue sarcoma (2015)

[a] www.ncbi.nlm.nih.gov/pccompound.
[b] No. of hydrogen bond donors/acceptors.
[c] Calculated log of the partition coefficient as determined by MedChem Designer® v.1.0.1.15.
[d] See Ref. [67].
[e] GIST, gastrointestinal stromal tumor, HCC, Hepatocellular carcinoma, RCC, renal cell carcinoma.
[f] www.brimr.org/PKI/PKIs.htm.
[g] From Ref. [68].

oxygen. Moreover, the β3-lysine makes salt bridges with both the αC-E885 and DFG-D1046 (Fig. 8A). The drug makes hydrophobic contact with the β1-strand L840 just before the G-rich loop, the β2 V848 (CS7) distal to the G-rich loop, the β3 A866 (CS8) and K868, L889 (RS3), V899 (Sh1) of the αC-β4 (back) loop, V914 of the β5-strand, the V916 gatekeeper (Sh2), L1035 (CS6) of the β7-strand, the C1045 just before the activation segment, and DFG-F1047 (RS2). The proximal pyridylvinyl moiety extends into the solvent while the distal benzamide moiety occupies BP-I-B in the gate area and the *N*-methyl group of benzamide is found within the back cleft (http://klifs.vu-compmedchem.nl/; PDB ID: 4AGC; note that this valuable searchable and noncommercial web site provides a comprehensive summary of drug and ligand binding to more than 1200 human and mouse protein kinases [83]). Axitinib is also a Kit and PDGFRβ antagonist and its effectiveness against RCC may be due to the co-inhibition of these enzymes, which promote cell growth and proliferation.

We have previously classified protein-kinase inhibitors based upon the nature of the structures of the drug-protein complexes [67]. Type I inhibitors bind in the active site cleft of the active enzyme form while type II inhibitors bind to the inactive DGF-D_{out} enzyme. Type III and type IV inhibitors are allosteric in nature; the former binds next to the ATP-binding site and the latter binds elsewhere. An advantage of allosteric inhibitors is that they cannot be

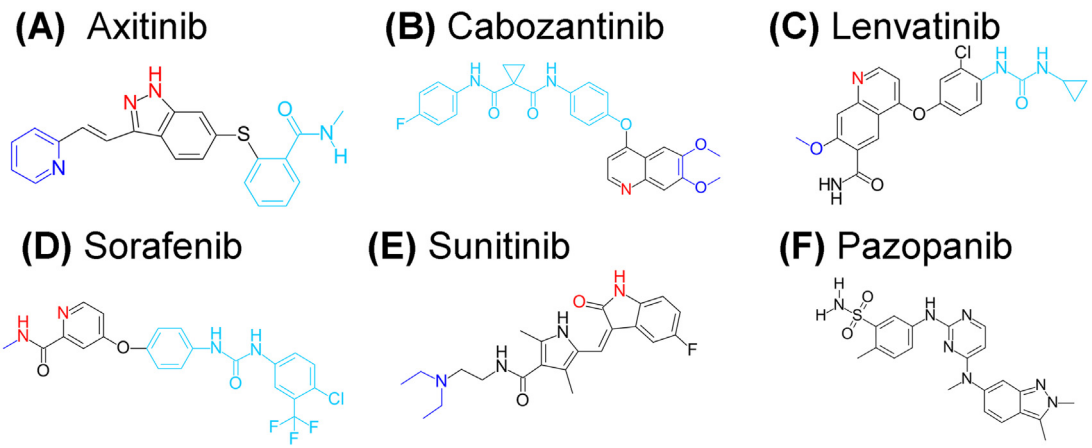

Fig. 7. Structures of all FDA-approved small molecule VEGFR inhibitors. The red letters denote atoms that make hydrogen bonds with hinge residues, the sky blue lines indicate residues that reside in hydrophobic pockets, and the dark blue lines indicate residues that extend from the enzyme into the solvent.

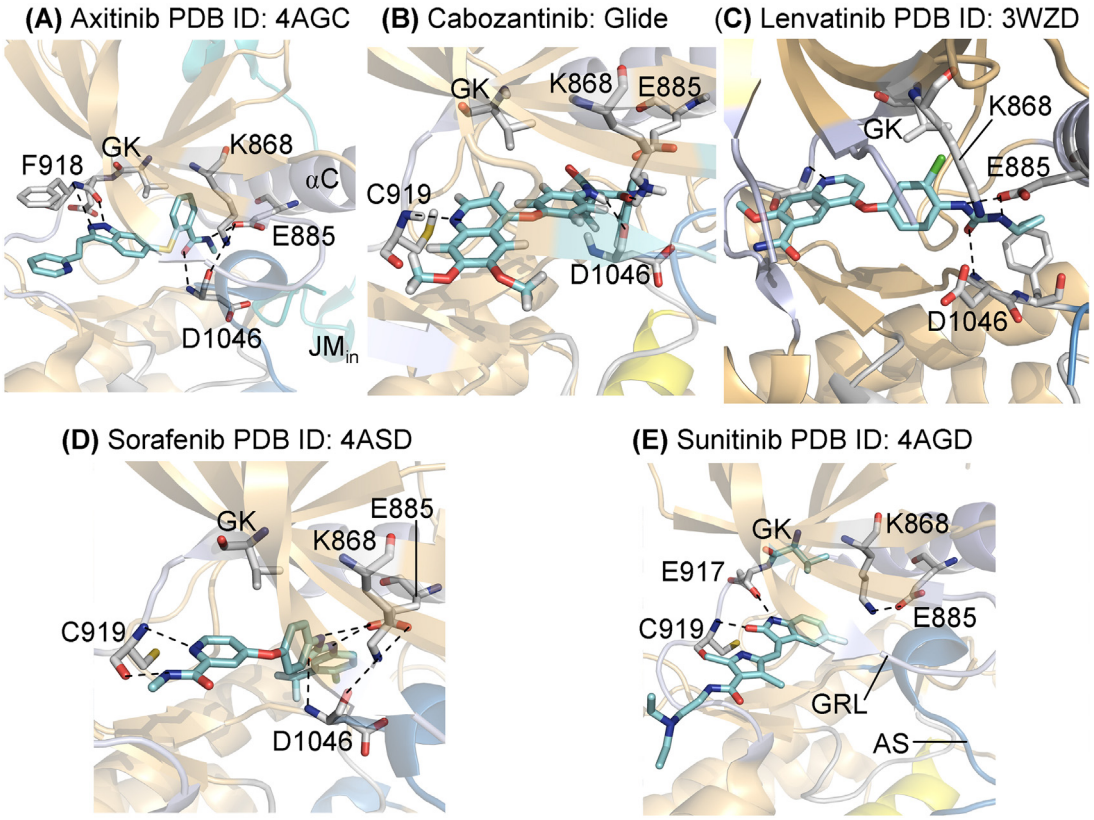

Fig. 8. Structures of drug-VEGFR2 complexes. The protein data base identification numbers are given and the Schrödinger program Glide [86] (Version 2016-1) was used to prepare (B). GK is the gatekeeper (Sh2) V916. Dashed lines represent polar bonds.

displaced by ATP whereas the inhibitory power of those antagonists that bind within the ATP-binding pocket can be overcome with high ATP concentrations. Type V inhibitors are bivalent and bind to two portions of the protein kinase domain and Type VI inhibitors form a covalent bond with the enzyme. Zuccotto et al. introduced type I1/2 inhibitors as those antagonists that bind to dormant enzymes with the DGF-D_{in} structure [85]. The type I1/2 and type II inhibitors are subclassified into type A and B where the type A inhibitors extend past the gatekeeper residue toward the αC-helix and occupy portions of the gate area and back cleft including BP-I-A, BP-I-B, BP-II-A, BP-II-B [83,84] while the type B inhibitors do not extend into the back cleft. The back cleft roughly corresponds to the RDP of McTigue et al. [68]. Preliminary data suggest that the type A inhibitors have a long residence time while the type B inhibitors have a short residence time [67]. Axitinib is bound to a DFG-D_{out} VEGFR2 conformation and extends into the back pocket thereby classifying it as a type IIA inhibitor. McTigue et al. note that the drug extends to the edge of JM_{in} where it makes van der Waals contact with I804 within the JM segment [68].

Cabozantinib is FDA-approved as a second-line treatment for metastatic renal cell carcinomas (Table 5). There are no VEGFR2-cabozantinib structures in the public domain and we used the Schrödinger Glide program [86] to generate models of such drug-enzyme interactions beginning with the VEGFR2 PDB ID: 4ASD as a template. The result indicates that the antagonist is also a type IIA inhibitor of VEGFR2 protein-tyrosine kinase. The pose shows

that the quinoline *N*1 (Fig. 7B) forms a hydrogen bond with the N—H group of the C919 within the hinge. One carbonyl group next to the cyclopropane forms a hydrogen bond with the β3-K868 (Fig. 8B) and the amino group attached to the oxyphenyl moiety forms a hydrogen bond with the carbonyl group of DFG-D1046. The drug makes hydrophobic contact with L840 immediately before the G-rich loop, V848 (CS7), A866 (CS8), and I888, L889, and I892 within the αC-helix, V899 (Sh1) within the αC-β4 loop, the V916 gatekeeper (Sh2), L1019 and I1025 before the catalytic loop, HRD-H1026 (RS1), L1035 (CS6), and DFG-F1047 (RS2). The two methoxy groups extend into the solvent. Cabozantinib is bound to a DFG-D_{out} VEGFR2 conformation and extends into the back pocket thereby classifying it as a type IIA inhibitor. The template 4ASD has a JM_{out} configuration and the superposition of the model pose with 4AGD (JM_{in}) indicates that there would be a steric clash of cabozantinib with JM_{in}. This medicinal is a multi-kinase inhibitor (Table 5) [87] and it is likely that its therapeutic effectiveness may be related to enzymes besides VEGFR1/2/3.

Lenvatinib is a type I½A inhibitor of VEGFR2 that is approved as part of a dual therapy with everolimus (an allosteric type IV mTOR inhibitor) for the treatment of metastatic RCC that has previously been treated with one prior anti-angiogenic regimen (Table 5) [88]. The X-ray structure indicates that *N*1 of the lenvatinib quinoline group (Fig. 7C) forms a hydrogen bond with the hinge C919 N—H group [89]. The αC-E885 forms a hydrogen bond with each N—H group of the lenvatinib urea moiety and the N—H group of DFG-D1046 forms a hydrogen bond with the urea carbonyl group (Fig. 8C). Furthermore, lenvatinib makes hydrophobic contacts with L840 within the G-rich loop, V848 (CS7), the β3 A866 (CS8) and K868, I888 and the L889 (RS3) of the αC-helix, V899 (Sh1) of the αC-β4 loop, V796 and F798 of the hinge, L1035 (CS6), C1045 before the activation segment, DFG-F1047 (RS2), and L1049 within the activation segment. Furthermore, the DFG-D1046 of makes van der Waals contact with the drug. The RS3/4 residues of the regulatory spine are displaced upward from RS2 indicating that the enzyme is inactive (not shown); the DFG-D points inward and the drug extends past the gatekeeper toward the αC-helix occupying BP-I-B and BP-II-in (klifs.vu-compmedchem.nl; PDB ID 3WZD). These properties are those of a type I½A inhibitor [67]. Lenvatinib is also an inhibitor of FGFR1/2/3/4, Kit, PDGFRα, and RET and its effectiveness may be related to the inhibition of more than VEGFR1/2/3.

Sorafenib is a VEGFR1/2/3 protein-tyrosine kinase antagonist that was approved for the first-line treatment of metastatic renal cell carcinomas (Table 5). The X-ray crystal structure indicates that the pyridine *N*1 of sorafenib (Fig. 7D) forms a hydrogen bond with the N—H of C919 of the hinge and the amide N—H group of the drug forms a hydrogen bond with the C919 carbonyl group. αC-E885 forms a hydrogen bond with one of the urea N—H groups and the urea oxygen forms a hydrogen bond with the N—H group of DFG-D1046 (Fig. 8D). The drug also makes hydrophobic contacts with the β1-strand L840 before the G-rich loop, V848 (CS7) after the G-rich loop, the β3 A866 (CS8) and K868, L889 (RS3), I892 within the αC-helix, V899 (Sh1) within the αC-β4 loop, the V916 gatekeeper (Sh2), F918 of the hinge, L1019 before the catalytic loop, HRD-H1026 (RS1) of the catalytic loop, the β7-strand L1035 (CS6), I1044 and C1045 just before the activation segment, and DFG-F1047 (RS2). Sorafenib binds to the BP-I-B, BP-II out, and BP-III sub-pockets in the gate area and the back cleft of VEGFR2. The DFG-D1046 is pointed away from the active site and the drug extends past the gatekeeper toward the αC-helix indicating that the drug is a type IIA inhibitor [67]. This drug is a multi-kinase inhibitor [90] and is also approved for the treatment of hepatocellular and thyroid carcinomas.

Sunitinib is an FDA-approved medication for the first-line treatment of renal cell carcinomas. The X-ray structure indicates that the N—H group of the sunitinib indolinone scaffold (Fig. 7E) forms one hydrogen bond with the E917 hinge carbonyl group and the ketone oxygen of the scaffold forms a second hydrogen bond with the N—H group of C919 of the VEGFR2 hinge (Fig. 8E) [68]. The drug also makes hydrophobic contacts with the β1-strand L840, A866 (CS8), V899 (Sh1) of the αC-β4 loop, the V916 gatekeeper (Sh2), F918 of the hinge, L1035 (CS6), C1054 just before the activation segment, and DFG-F1047 (RS2). The DFG-D1046 is directed away from the active site and the drug does not extend past the gatekeeper toward the αC-helix, which are properties of a type IIB inhibitor. The antagonist binds to a JM_{in} enzyme form (Fig. 4B). Renal cell carcinomas are highly vascular tumors and the effectiveness of sunitinib is ascribed in large part to the inhibition of VEGFR [91,92]. However, co-inhibition of PDGFRβ and Kit may potentiate its effect in the treatment of RCC.

Pazopanib is approved as a first-line treatment for advanced renal cell carcinomas (Table 5) [93]. There is no VEGFR2-pazopanib available in the public domain (www.rcsb.org/pdb/home/home.do). We attempted to generate a model *in silico* using the Schrödinger Glide and the Induced Fit programs [86,94], but we were unable to obtain a satisfactory structure. However, the description provided by McTigue et al. indicates that pazopanib is a type IIA inhibitor of VEGFR2 [68]. Like the other drugs mentioned above, pazopanib inhibits Kit and PDGFR in addition to VEGFR1/2/3 (Table 5). Moreover, it is possible or even likely that the adverse effects of the drugs mentioned in this section as well as their therapeutic effects are due to the inhibition of non-VEGFR protein kinases. However, it would be very difficult to differentiate therapeutic and adverse effects of multi-kinase inhibitors owing to the complexity of protein kinase signaling pathways.

3.2. Structure of the VEGF-A-bevacizumab complex

Bevacizumab, which is a humanized mouse monoclonal antibody directed against human VEGF-A, was approved in 2009 for the first-line treatment of renal cell carcinomas in conjunction with interferon-α. As a high molecular weight protein, the drug must be given intravenously, which is in contrast to the six orally effective small molecule inhibitors considered in the previous section. The formation of the VEGF-A–mAb complex prevents the binding of the factor to VEGFR1/2. Muller et al. reported that the X-ray crystal structure of VEGF-A closely resembles that found in the VEGF-A–antibody complex indicating that the mechanism of action of the antibody is unrelated to an induced VEGF-A conformational change [95]. The antibody binds to VEGF-A from residues ^{79}QIMRIKPHQGQHIGEM^{94}, which includes the β5-strand, the β5-β6 loop (L3), and the β6-strand of the growth factor.

Kim et al. prepared a mouse monoclonal antibody (Mab A4.6.1) directed against human VEGF-A, which inhibits cell signaling in animals *in vivo* [96]. A humanized antibody was prepared by site-directed mutagenesis that contains the antigen-binding residues of the mouse monoclonal antibody; moreover, the derivative antibody possesses an affinity for VEGF-A comparable to that of the original mouse antibody (K_d = 1.8 nM) [97]. The humanization of the antibody minimizes the likelihood that the protein will be rejected because of its antigenicity. Muller et al. measured the affinity of this antibody to wild type and alanine site-specific mutants of VEGF-A_{8-109} [95]. They found that residues in the VEGF-A β5-strand (Met81, Arg82, and Ile83), the β5-β6 loop (G88), and the β6-strand (Gln89 and Gly92) are essential in forming a high-affinity complex with the VEGF-A antigen-binding fragment (Fab). Each of these single mutants increases the IC_{50} from 22 to 107 fold [95]. The humanized antibody used in this study corresponds to bevacizumab (Avastin).

Muller et al. prepared 68 alanine mutants of the Fab fragment and compared the affinity of VEGF-A_{8-109} to the wild type and to the antigen-binding site mutants [95]. They identified eight Fab residues that play an important role in binding VEGF-A_{8-109}. A

Table 6
Location of VEGF-A_{8-109} residues that interact with Fab and VEGFR1/2.[a]

Structure	Residues	Fab	VEGFR1	VEGFR2
α1	16–24		Lys16, Phe17, Met18, Tyr21, Gln22	Phe17, Met18
α1-β1 turn	25–26		Tyr25	
β1	27–34		His27	
α2	35–42			
α2-β2 turn; L1[b]	43–45		Ile43	Ile43
β2	46–49		Lys48	Ile46, Phe47
β3	51–58			
β3-β4 loop; L2[b]	59–65		Cys61, Asn62, Asp63, Glu64, Gly65	Glu64
β4	67–69		Leu66	
β5	73–83	Met81, Arg82, Ile83	Gln79, Met81, Ile83	Gln79, Ile83
β5-β6 loop; L3[b]	84–88	Gly88	Pro85, His86,	Lys84, Pro85
β6	89–99	Gln89, Gly92	Ile91	
β7	100–106		Glu103, Cys104, Arg105, Pro106	

[a] Data from Ref. [95].
[b] L, Loop in VEGF-A_{8-109}.

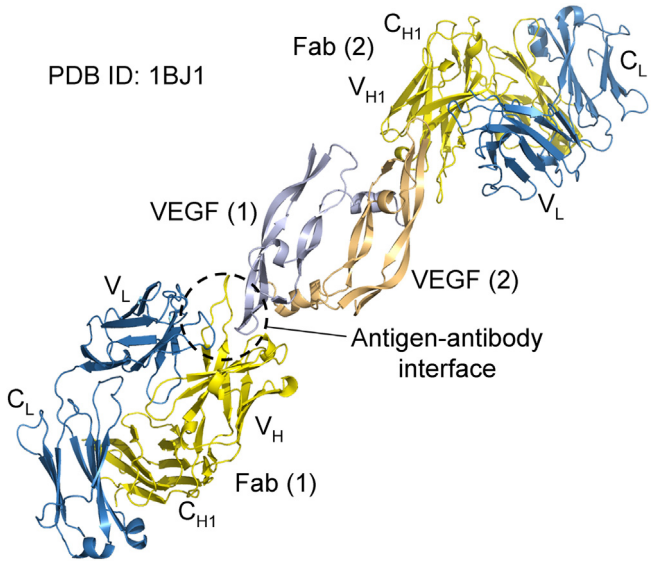

Fig. 9. Structure of the bevacizumab-VEGF-A complex. V_H, variable heavy chain; V_L, variable light chain; C_L, constant light chain; C_H, constant heavy chain. Fab, fragment antigen binding.

Trp96Ala mutation of the V_L (variable light) chain increases the IC_{50} by greater than 150 fold. Mutation of each of seven residues of the V_H (variable heavy) chain to Ala (Asn31, Tyr32, Trp50, Asn52, Tyr95, Ser106 and Trp108) increases the IC_{50} by greater than 150 fold [95]. The V_L chain contains three complementary determining regions (CDRs): L1, L2, and L3 (note that the L1, L2, L3 refer to the antibody and not to VEGF-A). The V_H chain also contains three CDRs: H1, H2, and H3.

The structure of the antigen-binding fragment (Fab) of bevacizumab complexed with VEGF-A_{8-109} was determined by X-ray crystallography [95] (Fig. 9). The overall conformation of VEGF-A_{8-109} bound to the Fab is very similar to the unbound molecule as previously described (Fig. 1). The β5-β6 loop of VEGF-A_{8-109} exhibits conformational flexibility in the free state and anti-VEGF-A_{8-109} selects and stabilizes one of the conformations. The functional epitope of VEGF-A_{8-109} is dominated by the six residues listed in Table 6. Each of these binding determinants of VEGF-A_{8-109} is in intimate contact with Fab.

A large proportion of antigen-binding residues of Fab are aromatic and hydrophobic in nature and this finding is a general property of antibody combining sites [95]. For example, Gly88 of VEGF-A_{8-109} interacts through an aromatic box formed by the side chains of residues Trp50 of CDR H2 along with Tyr99 and Trp108 of CDR H3. All of these residues are important binding determinants as demonstrated by alanine-scanning mutagenesis of Fab. Other important interactions include Met81 of VEGF-A_{8-109} and Tyr54 of CDR H2 along with Ile83 of VEGF-A_{8-109} and Asn52 of CDR H2. The side chain of VEGF-A_{8-109} Gln89 hydrogen bonds with the side chain of Thr53 of Fab while its carbonyl group forms another hydrogen bond with the Gly33 N—H group of Fab. There is a channel of water molecules buried between VEGF-A_{8-109} and $VEGFR2_{IgD2}$ [98] whereas there are no water molecules buried in the VEGF-A_{8-109} antigen-Fab interface [95]. The absence of water molecules is an indication of greater interaction specificity with the antibody.

Because the overall structure of free VEGF-A_{8-109} is nearly identical to that in the complex with the Fab fragment, the biological inhibitory effect of anti-VEGF is not the result of inducing a conformational change. Of the 16 residues of VEGF-A_{8-109} that occur at the antigen-Fab interface, nine also occur at the VEGF-A_{8-109}-$VEGFR1_{IgD2}$ interface. The inhibitory effect of this monoclonal antibody results from sterically blocking the interaction of VEGF-A with its receptors. In examining the identity of the VEGF-A_{8-109} residues that interact with VEGFR1, VEGFR2, and Fab (Table 6), only Ile83 is an important binding determinant for all three proteins. The portion of VEGF-A_{8-109} that binds to the antibody involves a small cluster of residues in the β5-β6 locale of a single subunit. In contrast, the portion of VEGF-A_{8-109} that binds to VEGFR1/2 involves four different regions from each of the VEGF-A_{8-109} monomers: (i) an α1-helix and (ii) a β3-β4 loop of one VEGF-A_{8-109} monomer interacts with one VEGFR1/2 whereas (iii) a β2-strand and (iv) a β5-strand and β5-β6 loop from the same VEGF-A_{8-109} monomer interact with the its VEGFR1/2 dimeric partner. Additionally, the β7-strand of VEGF-A_{8-109} interacts with VEGFR1 (Table 6). Bevacizumab was FDA-approved for the treatment of metastatic colorectal cancer in 2004 [99]. It was subsequently approved for the treatment of metastatic non-squamous non-small cell lung cancer, glioblastoma, and ovarian and fallopian tumors. Common side effects include headache, hypertension, nose bleeds, and rash. Recall that hypertension is also a common side effect of the orally effective VEGFR inhibitors.

3.3. Clinical trials

Prior to the advent of drugs that target VEGF-A and VEGFR1/2/3, there were no effective therapies for renal cell carcinomas [100–103]. Bevacizumab was approved for the treatment of this malady in 2009. Beginning with sorafenib in 2005, a half dozen small molecule VEGFR inhibitors have found their way to the clinic (www.brimr.org/PKI/PKIs.htm) [104]. Like most other protein kinase inhibitors, progression-free responses last on the order of one year. Current clinical studies are directed toward determining

the best first-line treatments and then subsequent follow-up treatments when resistance becomes apparent. Unfortunately, there are no biomarkers that are correlated with effective treatment outcomes or drug toxicity. Biomarkers that have been studied include plasma levels of cytokines, VHL mutational status, and gene expression profiling. One of the more common adverse effects in response to the orally effective drugs that target VEGFR protein kinase activity is hypertension. Moreover, there is a positive correlation between RCC treatment effectiveness and the occurrence of hypertension. Other side effects produced by the anti-angiogenic drugs include decreased appetite, weight loss, fatigue, and gastrointestinal upsets (nausea, vomiting, and diarrhea) [103]. In addition to these VEGF-A targeted therapies, the immune checkpoint inhibitor nivolumab, which is directed against PD-1, has been approved as a second-line treatment for RCC. Its side effects parallel those observed for the targeted protein kinase inhibitors. See Refs. [99–103] for a summary of the clinical trials that led to the approval of bevacizumab and the drugs listed in Table 5; see Ref. [105] for a summary of the studies that led to the approval of nivolumab.

4. Epilogue

Maharaj et al. surveyed the expression of VEGF-A and VEGFR2 in the adult mouse [106]. They found that VEGF-A is expressed in all vascularized organs and tissues. It was expressed in close proximity to fenestrated blood vessels within endocrine glands, the choroid plexus, and kidney glomeruli. Fenestrae are the small pores in endothelial cells that allow for the transfer of small molecules and proteins with the surrounding tissue. In general VEGF-A is not expressed by endothelial cells, but rather by cells such as pericytes that are adjacent to endothelial cells; this expression pattern is in agreement with the notion that the factor functions in a paracrine fashion. The VEGF family of factors is also expressed by tumor cells and tumor cell stroma. Using phosphospecific antibodies, Maharaj et al. found that VEGFR2 was in an activated state in all vascularized organs. Because endothelial cells are generally quiescent, these findings suggest that VEGF-A and its receptors play an important role in addition to endothelial cell mitogenesis, namely endothelial cell survival and permeability.

In contrast to the normal vasculature, tumor vessels are leaky [107]. This is due in part to the abundant expression of VEGF-A with its permeability enhancing activities. The fibroblast growth factors are also able to stimulate angiogenesis *in vitro*. FGF2, which stimulates endothelial cell growth and division, was discovered and characterized before VEGF-A [108], but the angiogenic role of the more than 20 FGFs and FGFR1/2/3/4 *in vivo* is unclear. The over activity of PDGF and PDGFR family has been linked to tumor progression. PDGFR-β is expressed in tumor pericytes and preclinical and clinical studies suggest that inhibitors targeting both VEGFR and PDGFR may be more beneficial than targeting only VEGFR [104,109].

Many patients with metastatic renal cell carcinoma do not respond to targeted VEGFR antagonists and those who do respond usually experience tumor progression within one year [101]. In contrast to the resistance sparked by the targeted ALK or EGFR inhibitors in the treatment of lung cancers due to mutations in the receptor [8,64,65], there is no evidence that mutations in VEGF-A or VEGFR2 are responsible for the development of resistance to the VEGF and VEGFR inhibitors [99]. One likely reason for the development of resistance following targeted anti-VEGF or anti-VEGFR treatment in RCC may be to the increased production of pro-angiogenic factors such as the fibroblast growth factors or the platelet-derived growth factors. Deciphering the mechanisms responsible for resistance is further complicated by the occurrence of several dozen physiological pro- and anti-angiogenic factors whose activities may change in response to anti-angiogenic agents [6]. As noted by Winer et al. “Biologically, the cancer cell is notoriously wily; each time we throw an obstacle in its path, it finds an alternate route that must then be blocked” [110]. However, combinations of drugs that inhibit tumor cell growth and division coupled with anti-angiogenic agents may prove to be efficacious in the long term treatment of renal cell carcinomas as well as other cancers. Owing to the resistance of renal cell carcinomas to cytotoxic drugs and radiation therapy, the development of anti-angiogenic agents has greatly improved the therapeutic options in the treatment of these malignancies.

Acknowledgments

The colored figures in this paper were checked to ensure that their perception was accurately conveyed to colorblind readers [111]. The author thanks Laura M. Roskoski for providing editorial and bibliographic assistance.

References

[1] R.L. Siegel, K.D. Miller, A. Jemal, Cancer statistics, 2017, CA Cancer J. Clin. 67 (2017) 7–30.
[2] H.T. Cohen, F.J. McGovern, Renal-cell carcinoma, N. Engl. J. Med. 353 (2005) 2477–2490.
[3] H.I. Scher, R.J. Motzer, Bladder and renal cell carcinomas, in: D.L. Longo, D.L. Kasper, J.L. Jameson, A.S. Fauci, S.L. Hauser, J. Loscalzo (Eds.), Harrison's Principles of Internal Medicine, 18th edition, McGraw Hill Medical, New York, 2012, pp. 790–795.
[4] E. Jonasch, J. Gao, W.K. Rathmell, Renal cell carcinoma, BMJ 349 (2014) g4797.
[5] C.E. Alpers, A. Chang, The kidney, in: V. Kumar, A.K. Abbas, J.C. Aster (Eds.), Robbins and Cotran Pathologic Basis of Disease, ninth ed., Elsevier Saunders, Philadelphia, 2015, pp. 952–956.
[6] R. Roskoski Jr., Vascular endothelial growth factor (VEGF) signaling in tumor progression, Crit. Rev. Oncol. Hematol. 62 (2007) 179–213.
[7] R. Roskoski Jr., Anaplastic lymphoma kinase (ALK): structure, oncogenic activation, and pharmacological inhibition, Pharmacol. Res. 68 (2013) 68–94.
[8] R. Roskoski Jr., The preclinical profile of crizotinib for the treatment of non-small-cell lung cancer and other neoplastic disorders, Expert Opin. Drug Discov. 8 (2013) 1165–1179.
[9] D. Hanahan, J. Folkman, Patterns and emerging mechanisms of the angiogenic switch during tumorigenesis, Cell 86 (1996) 353–364.
[10] N. Ferrara, Vascular endothelial growth factor: basic science and clinical progress, Endocr. Rev. 25 (2004) 581–611.
[11] J. Folkman, Tumor angiogenesis: therapeutic implications, N. Engl. J. Med. 285 (1971) 1182–1186.
[12] L. Eklund, B.R. Olsen, Tie receptors and their angiopoietin ligands are context-dependent regulators of vascular remodeling, Exp. Cell Res. 312 (2006) 630–641.
[13] M. Heroult, F. Schaffner, H.G. Augustin, Eph receptor and ephrin ligand-mediated interactions during angiogenesis and tumor progression, Exp. Cell Res. 312 (2006) 642–650.
[14] M. Relf, S. LeJeune, P.A. Scott, S. Fox, K. Smith, R. Leek, et al., Expression of the angiogenic factors vascular endothelial cell growth factor, acidic and basic fibroblast growth factor, tumor growth factor β-1, platelet-derived endothelial cell growth factor, placenta growth factor, and pleiotrophin in human primary breast cancer and its relation to angiogenesis, Cancer Res. 57 (1997) 963–969.
[15] H.F. Guo, C.W. Vander Kooi, Neuropilin functions as an essential cell surface receptor, J. Biol. Chem. 290 (2015) 29120–29126.
[16] M.S. O'Reilly, L. Holmgren, Y. Shing, C. Chen, R.A. Rosenthal, M. Moses, et al., Angiostatin: a novel angiogenesis inhibitor that mediates the suppression of metastases by a Lewis lung carcinoma, Cell 79 (1994) 315–328.
[17] M.S. O'Reilly, T. Boehm, Y. Shing, N. Fukai, G. Vasios, W.S. Lane, et al., Endostatin: an endogenous inhibitor of angiogenesis and tumor growth, Cell 88 (1997) 277–285.
[18] K.M. Dameron, O.V. Volpert, M.A. Tainsky, N. Bouck, Control of angiogenesis in fibroblasts by p53 regulation of thrombospondin-1, Science 265 (1994) 1582–1584.
[19] A. Hoeben, B. Landuyt, M.S. Highley, H. Wildiers, A.T. Van Oosterom, E.A. De Bruijn, Vascular endothelial growth factor and angiogenesis, Pharmacol. Rev. 56 (2004) 549–580.
[20] D.R. Senger, S.J. Galli, A.M. Dvorak, C.A. Perruzzi, V.S. Harvey, H.F. Dvorak, Tumor cells secrete a vascular permeability factor that promotes accumulation of ascites fluid, Science 219 (1983) 983–985.
[21] N. Ferrara, W.J. Henzel, Pituitary follicular cells secrete a novel heparin-binding growth factor specific for vascular endothelial cells, Biochem. Biophys. Res. Commun. 161 (1989) 851–858.

[22] D.T. Connolly, D.M. Heuvelman, R. Nelson, J.V. Olander, B.L. Eppley, J.J. Delfino, et al., Tumor vascular permeability factor stimulates endothelial cell growth and angiogenesis, J. Clin. Invest. 84 (1989) 1470–1478.
[23] D.W. Leung, G. Cachianes, W.J. Kuang, D.V. Goeddel, N. Ferrara, Vascular endothelial growth factor is a secreted angiogenic mitogen, Science 246 (1989) 1306–1309.
[24] Y.A. Muller, H.W. Christinger, B.A. Keyt, A.M. de Vos, The crystal structure of vascular endothelial growth factor (VEGF) refined to 1. 93 A resolution: multiple copy flexibility and receptor binding, Structure 5 (1997) 1325–1338.
[25] S. Iyer, P.D. Scotney, A.D. Nash, K. Ravi Acharya, Crystal structure of human vascular endothelial growth factor-B: identification of amino acids important for receptor binding, J. Mol. Biol. 359 (2006) 76–85.
[26] V.M. Leppänen, A.E. Prota, M. Jeltsch, A. Anisimov, N. Kalkkinen, T. Strandin, et al., Structural determinants of growth factor binding and specificity by VEGF receptor 2, Proc. Natl. Acad. Sci. U. S. A. 107 (2010) 2425–2430.
[27] V.M. Leppänen, M. Jeltsch, A. Anisimov, D. Tvorogov, K. Aho, N. Kalkkinen, et al., Structural determinants of vascular endothelial growth factor-D receptor binding and specificity, Blood 117 (2011) 1507–1515.
[28] S. Iyer, D.D. Leonidas, G.J. Swaminathan, D. Maglione, M. Battisti, M. Tucci, et al., The crystal structure of human placenta growth factor-1 (PlGF-1), an angiogenic protein, at 2.0 A resolution, J. Biol. Chem. 276 (2001) 12153–12161.
[29] M. Simons, E. Gordon, L. Claesson-Welsh, Mechanisms and regulation of endothelial VEGF receptor signalling, Nat. Rev. Mol. Cell. Biol. 17 (2016) 611–625.
[30] J. Lagercrantz, F. Farnebo, C. Larsson, T. Tvrdik, G. Weber, F. Piehl, A comparative study of the expression patterns for *vegf*, *vegf-b/vrf* and *vegf-c* in the developing and adult mouse, Biochim. Biophys. Acta 1398 (1998) 157–163.
[31] H.M. Bui, D. Enis, M.R. Robciuc, H.J. Nurmi, J. Cohen, M. Chen, et al., Proteolytic activation defines distinct lymphangiogenic mechanisms for VEGFC and VEGFD, J. Clin. Invest. 126 (2016) 2167–2180.
[32] A. Aspelund, M.R. Robciuc, S. Karaman, T. Makinen, K. Alitalo, Lymphatic system in cardiovascular medicine, Circ. Res. 118 (2016) 515–530.
[33] A.K. Olsson, A. Dimberg, J. Kreuger, L. Claesson-Welsh, VEGF receptor signalling—in control of vascular function, Nat. Rev. Mol. Cell Biol. 7 (2006) 359–371.
[34] S. Ogawa, A. Oku, A. Sawano, S. Yamaguchi, Y. Yazaki, M. Shibuya, A novel type of vascular endothelial growth factor, VEGF-E (NZ-7 VEGF), preferentially utilizes KDR/Flk-1 receptor and carries a potent mitotic activity without heparin-binding domain, J. Biol. Chem. 273 (1998) 31273–31282.
[35] K. Suto, Y. Yamazaki, T. Morita, H. Mizuno, Crystal structures of novel vascular endothelial growth factors (VEGF) from snake venoms: insight into selective VEGF binding to kinase insert domain-containing receptor but not to fms-like tyrosine kinase-1, J. Biol. Chem. 280 (2005) 2126–2131.
[36] M. Shibuya, S. Yamaguchi, A. Yamane, T. Ikeda, A. Tojo, H. Matsushime, M. Sato, Nucleotide sequence and expression of a novel human receptor-type tyrosine kinase gene (flt) closely related to the fms family, Oncogene 5 (1990) 519–524.
[37] W. Matthews, C.T. Jordan, M. Gavin, N.A. Jenkins, N.G. Copeland, I.R. Lemischka, A receptor tyrosine kinase cDNA isolated from a population of enriched primitive hematopoietic cells and exhibiting close genetic linkage to c-kit, Proc. Natl. Acad. Sci. U. S. A. 88 (1991) 9026–9030.
[38] B.I. Terman, M.E. Carrion, E. Kovacs, B.A. Rasmussen, R.L. Eddy, T.B. Shows, Identification of a new endothelial cell growth factor receptor tyrosine kinase, Oncogene 6 (1991) 1677–1683.
[39] B.I. Terman, M. Dougher-Vermazen, M.E. Carrion, D. Dimitrov, D.C. Armellino, D. Gospodarowicz, P. Bohlen, Identification of the KDR tyrosine kinase as a receptor for vascular endothelial cell growth factor, Biochem. Biophys. Res. Commun. 187 (1992) 1579–1586.
[40] W.J. Fantl, D.E. Johnson, L.T. Williams, Signalling by receptor tyrosine kinases, Annu. Rev. Biochem. 62 (1993) 453–481.
[41] G.H. Fong, J. Rossant, M. Gertsenstein, M.L. Breitman, Role of the Flt-1 receptor tyrosine kinase in regulating the assembly of vascular endothelium, Nature 376 (1995) 66–70.
[42] F. Shalaby, J. Rossant, T.P. Yamaguchi, M. Gertsenstein, X.F. Wu, M.L. Breitman, A.C. Schuh, Failure of blood-island formation and vasculogenesis in Flk-1-deficient mice, Nature 376 (1995) 62–66.
[43] D.J. Dumont, L. Jussila, J. Taipale, A. Lymboussaki, T. Mustonen, K. Pajusola, et al., Cardiovascular failure in mouse embryos deficient in VEGF receptor-3, Science 282 (1998) 946–949.
[44] R.L. Kendall, K.A. Thomas, Inhibition of vascular endothelial cell growth factor activity by an endogenously encoded soluble receptor, Proc. Natl. Acad. Sci. U. S. A. 90 (1993) 10705–10709.
[45] D.E. Clark, S.K. Smith, Y. He, K.A. Day, D.R. Licence, A.N. Corps, et al., A vascular endothelial growth factor antagonist is produced by the human placenta and released into the maternal circulation, Biol. Reprod. 59 (1998) 1540–1548.
[46] C.J. Robinson, D.D. Johnson, E.Y. Chang, D.M. Armstrong, W. Wang, Evaluation of placenta growth factor and soluble Fms-like tyrosine kinase 1 receptor levels in mild and severe preeclampsia, Am. J. Obstet. Gynecol. 195 (2006) 255–259.
[47] J.E. Park, H.H. Chen, J. Winer, K.A. Houck, N. Ferrara, Placenta growth factor. Potentiation of vascular endothelial growth factor bioactivity, *in vitro* and *in vivo*, and high affinity binding to Flt-1 but not to Flk-1/KDR, J. Biol. Chem. 269 (25) (1994) 646–654.
[48] J.M. Ebos, G. Bocci, S. Man, P.E. Thorpe, D.J. Hicklin, D. Zhou, et al., A naturally occurring soluble form of vascular endothelial growth factor receptor 2 detected in mouse and human plasma, Mol. Cancer Res. 2 (2004) 315–326.
[49] J.M. Ebos, C.R. Lee, E. Bogdanovic, J. Alami, P. Van Slyke, G. Francia, et al., Vascular endothelial growth factor-mediated decrease in plasma soluble vascular endothelial growth factor receptor-2 levels as a surrogate biomarker for tumor growth, Cancer Res. 68 (2008) 521–529.
[50] M. Jeltsch, T. Karpanen, T. Strandin, K. Aho, H. Lankinen, K. Alitalo, Vascular endothelial growth factor (VEGF)/VEGF-C mosaic molecules reveal specificity determinants and feature novel receptor binding patterns, J. Biol. Chem. 281 (2006) 12187–12195.
[51] J. Solowiej, S. Bergqvist, M.A. McTigue, T. Marrone, T. Quenzer, M. Cobbs, et al., Characterizing the effects of the juxtamembrane domain on vascular endothelial growth factor receptor-2 enzymatic activity, autophosphorylation, and inhibition by axitinib, Biochemistry 48 (2009) 7019–7031.
[52] M.A. Lemmon, J. Schlessinger, Cell signaling by receptor tyrosine kinases, Cell 141 (2010) 1117–1134.
[53] R.L. Kendall, R.Z. Rutledge, X. Mao, A.J. Tebben, R.W. Hungate, K.A. Thomas, Vascular endothelial growth factor receptor KDR tyrosine kinase activity is increased by autophosphorylation of two activation loop tyrosine residues, J. Biol. Chem. 274 (1999) 6453–6460.
[54] S. Sarabipour, K. Ballmer-Hofer, K. Hristova, VEGFR-2 conformational switch in response to ligand binding, Elife 5 (2016) e13876, http://dx.doi.org/10.7554/eLife.13876.
[55] S.R. Hubbard, J.H. Till, Protein tyrosine kinase structure and function, Annu. Rev. Biochem. 69 (2000) 373–398.
[56] L. Wei, S.R. Hubbard, W.A. Hendrickson, L. Ellis, Expression, characterization, and crystallization of the catalytic core of the human insulin receptor protein-tyrosine kinase domain, J. Biol. Chem. 270 (1995) 8122–8130.
[57] R.D. Meyer, M. Mohammadi, N. Rahimi, A single amino acid substitution in the activation loop defines the decoy characteristic of VEGFR-1/FLT-1, J. Biol. Chem. 281 (2006) 867–875.
[58] A. Salameh, F. Galvagni, M. Bardelli, F. Bussolino, S. Oliviero, Direct recruitment of CRK and GRB2 to VEGFR-3 induces proliferation, migration, and survival of endothelial cells through the activation of ERK, AKT, and JNK pathways, Blood 106 (2005) 3423–3431.
[59] L.E. Locascio, D.J. Donoghue, KIDs rule: regulatory phosphorylation of RTKs, Trends Biochem. Sci. 38 (2013) 75–84.
[60] D.R. Knighton, J.H. Zheng, L.F. Ten Eyck, V.A. Ashford, N.H. Xuong, S.S. Taylor, et al., Crystal structure of the catalytic subunit of cyclic adenosine monophosphate-dependent protein kinase, Science 253 (1991) 407–414.
[61] D.R. Knighton, J.H. Zheng, L.F. Ten Eyck, N.H. Xuong, S.S. Taylor, J.M. Sowadski, Structure of a peptide inhibitor bound to the catalytic subunit of cyclic adenosine monophosphate-dependent protein kinase, Science 253 (1991) 414–420.
[62] S.S. Taylor, A.P. Kornev, Protein kinases: evolution of dynamic regulatory proteins, Trends Biochem. Sci. 36 (2011) 65–77.
[63] S.K. Hanks, T. Hunter, Protein kinases 6: The eukaryotic protein kinase superfamily: kinase (catalytic) domain structure and classification, FASEB J. 9 (1995) 576–596.
[64] R. Roskoski Jr., A historical overview of protein kinases and their targeted small molecule inhibitors, Pharmacol. Res. 100 (2015) 1–23.
[65] R. Roskoski Jr., The ErbB/HER family of protein-tyrosine kinases and cancer, Pharmacol. Res. 79 (2014) 34–74.
[66] R. Roskoski Jr., Src protein-tyrosine kinase structure, mechanism, and small molecule inhibitors, Pharmacol. Res. 94 (2015) 9–25.
[67] R. Roskoski Jr., Classification of small molecule protein kinase inhibitors based upon the structures of their drug-enzyme complexes, Pharmacol. Res. 103 (2016) 26–48.
[68] M. McTigue, B.W. Murray, J.H. Chen, Y.L. Deng, J. Solowiej, R.S. Kania, Molecular conformations, interactions, and properties associated with drug efficiency and clinical performance among VEGFR TK inhibitors, Proc. Natl. Acad. Sci. U. S. A. 109 (2012) 18281–18289.
[69] F. Galvagni, S. Pennacchini, A. Salameh, M. Rocchigiani, F. Neri, M. Orlandini, et al., Endothelial cell adhesion to the extracellular matrix induces c-Src-dependent VEGFR-3 phosphorylation without the activation of the receptor intrinsic kinase activity, Circ. Res. 106 (2010) 1839–1848.
[70] S. Manni, K. Kisko, T. Schleier, J. Missimer, K. Ballmer-Hofer, Functional and structural characterization of the kinase insert and the carboxy terminal domain in VEGF receptor 2 activation, FASEB J. 28 (2014) 4914–4923.
[71] R. Roskoski Jr., ERK1/2 MAP kinases: structure, function, and regulation, Pharmacol. Res. 66 (2012) 105–143.
[72] M. Bry, R. Kivelä, V.M. Leppänen, K. Alitalo, Vascular endothelial growth factor-B in physiology and disease, Physiol. Rev. 94 (2014) 779–794.
[73] L. Muhl, C. Moessinger, M.Z. Adzemovic, M.H. Dijkstra, I. Nilsson, M. Zeitelhofer, et al., Expression of vascular endothelial growth factor (VEGF)-B and its receptor (VEGFR1) in murine heart, lung and kidney, Cell Tissue Res. 365 (2016) 51–63.
[74] S. Koch, S. Tugues, X. Li, L. Gualandi, L. Claesson-Welsh, Signal transduction by vascular endothelial growth factor receptors, Biochem. J. 437 (2011) 169–183.
[75] A. Álvarez-Aznar, L. Muhl, K. Gaengel, VEGF receptor tyrosine kinases: key regulators of vascular function, Curr. Top. Dev. Biol. 123 (2017) 433–482.

[76] A.P. Kornev, N.M. Haste, S.S. Taylor, L.F. Ten Eyck, Surface comparison of active and inactive protein kinases identifies a conserved activation mechanism, Proc. Natl. Acad. Sci. U. S. A. 103 (2006) 17783–17788.
[77] A.P. Kornev, S.S. Taylor, L.F. Ten Eyck, A helix scaffold for the assembly of active protein kinases, Proc. Natl. Acad. Sci. U. S. A. 105 (2008) 14377–14382.
[78] R. Roskoski Jr., Ibrutinib inhibition of Bruton protein-tyrosine kinase (BTK) in the treatment of B cell neoplasms, Pharmacol. Res. 113 (2016) 395–408.
[79] R. Roskoski Jr., Janus kinase (JAK) inhibitors in the treatment of inflammatory and neoplastic diseases, Pharmacol. Res. 111 (2016) 784–803.
[80] R. Roskoski Jr., Cyclin-dependent protein kinase inhibitors including palbociclib as anticancer drugs, Pharmacol. Res. 107 (2016) 249–275.
[81] R. Roskoski Jr., Allosteric MEK1/2 inhibitors including cobimetanib and trametinib in the treatment of cutaneous melanomas, Pharmacol. Res. 117 (2017) 20–31.
[82] H.S. Meharena, P. Chang, M.M. Keshwani, K. Oruganty, A.K. Nene, N. Kannan, et al., Deciphering the structural basis of eukaryotic protein kinase regulation, PLoS Biol. 11 (2013) e1001680.
[83] O.P. van Linden, A.J. Kooistra, R. Leurs, I.J. de Esch, C. de Graaf, KLIFS: a knowledge-based structural database to navigate kinase-ligand interaction space, J. Med. Chem. 57 (2014) 249–277.
[84] J.J. Liao, Molecular recognition of protein kinase binding pockets for design of potent and selective kinase inhibitors, J. Med. Chem. 50 (2007) 409–424.
[85] F. Zuccotto, E. Ardini, E. Casale, M. Angiolini, Through the gatekeeper door: exploiting the active kinase conformation, J. Med. Chem. 53 (2010) 2681–2694.
[86] R.A. Friesner, J.L. Banks, R.B. Murphy, T.A. Halgren, J.J. Klicic, D.T. Mainz, et al., Glide: a new approach for rapid, accurate docking and scoring: 1. Method and assessment of docking accuracy, J. Med. Chem. 47 (2004) 1739–1749.
[87] Y. Zhang, F. Guessous, A. Kofman, D. Schiff, R. Abounader, XL-184, a MET, VEGFR-2 and RET kinase inhibitor for the treatment of thyroid cancer, glioblastoma multiforme and NSCLC, IDrugs 13 (2010) 112–121.
[88] Z. Hussein, H. Mizuo, S. Hayato, M. Namiki, R. Shumaker, Clinical pharmacokinetic and pharmacodynamic profile of lenvatinib, an orally active, small-molecule, multitargeted tyrosine kinase inhibitor, Eur. J. Drug Metab. Pharmacokinet. (2017), http://dx.doi.org/10.1007/s13318-017-0403-4.
[89] K. Okamoto, M. Ikemori-Kawada, A. Jestel, K. von König, Y. Funahashi, T. Matsushima, et al., Distinct binding mode of multikinase inhibitor lenvatinib revealed by biochemical characterization, ACS Med. Chem. Lett. 6 (2014) 89–94.
[90] T. Ahmad, T. Eisen, Kinase inhibition with BAY 43-9006 in renal cell carcinoma, Clin. Cancer Res. 10 (2004) 6388S–6392S.
[91] R. Roskoski Jr., Sunitinib: a VEGF and PDGF receptor protein kinase and angiogenesis inhibitor, Biochem. Biophys. Res. Commun. 356 (2007) 323–328.
[92] R. Roskoski Jr., VEGF receptor protein-tyrosine kinases: structure and regulation, Biochem. Biophys. Res. Commun. 375 (2008) 287–291.
[93] G. Sonpavde, T.E. Hutson, Pazopanib: a novel multitargeted tyrosine kinase inhibitor, Curr. Oncol. Rep. 9 (2007) 115–119.
[94] W. Sherman, T. Day, M.P. Jacobson, R.A. Friesner, R. Farid, Novel procedure for modeling ligand/receptor induced fit effects, J. Med. Chem. 49 (2006) 534–553.
[95] Y.A. Muller, Y. Chen, H.W. Christinger, B. Li, B.C. Cunningham, H.B. Lowman, et al., VEGF and the Fab fragment of a humanized neutralizing antibody: crystal structure of the complex at 2.4 A resolution and mutational analysis of the interface, Structure 6 (1998) 1153–1167.
[96] K.J. Kim, B. Li, J. Winer, M. Armanini, N. Gillett, H.S. Phillips, N. Ferrara, Inhibition of vascular endothelial growth factor-induced angiogenesis suppresses tumour growth *in vivo*, Nature 362 (1993) 841–844.
[97] L.G. Presta, H. Chen, S.J. O'Connor, V. Chisholm, Y.G. Meng, L. Krummen, et al., Humanization of an anti-vascular endothelial growth factor monoclonal antibody for the therapy of solid tumors and other disorders, Cancer Res. 57 (1997) 4593–4599.
[98] C. Wiesmann, G. Fuh, H.W. Christinger, C. Eigenbrot, J.A. Wells, A.M. de Vos, Crystal structure at 1. 7 A resolution of VEGF in complex with domain 2 of the Flt-1 receptor, Cell 91 (1997) 695–704.
[99] N. Ferrara, A.P. Adamis, Ten years of anti-vascular endothelial growth factor therapy, Nat. Rev. Drug Discov. 15 (2016) 385–403.
[100] B.I. Rini, M.B. Atkins, Resistance to targeted therapy in renal-cell carcinoma, Lancet Oncol. 10 (2009) 992–1000.
[101] H. Zahoor, B.I. Rini, Emerging growth factor receptor antagonists for the treatment of renal cell carcinoma, Expert Opin. Emerg. Drugs 21 (2016) 431–440.
[102] C. Randrup Hansen, D. Grimm, J. Bauer, M. Wehland, N.E. Magnusson, Effects and side effects of using sorafenib and sunitinib in the treatment of metastatic renal cell carcinoma, Int. J. Mol. Sci. (2017) (pii: E461).
[103] K. Zarrabi, C. Fang, S. Wu, New treatment options for metastatic renal cell carcinoma with prior anti-angiogenesis therapy, J. Hematol. Oncol. 10 (2017) 38, http://dx.doi.org/10.1186/s13045-016-0374-y.
[104] P.M. Fischer, Approved and experimental small-molecule oncology kinase inhibitor drugs: a mid-2016 overview, Med. Res. Rev. 37 (2017) 314–367.
[105] M.C. Ornstein, B.I. Rini, The safety and efficacy of nivolumab for the treatment of advanced renal cell carcinoma, Expert Rev. Anticancer Ther. 16 (2016) 577–584.
[106] A.S. Maharaj, M. Saint-Geniez, A.E. Maldonado, P.A. D'Amore, Vascular endothelial growth factor localization in the adult, Am. J. Pathol. 168 (2006) 639–648.
[107] L. Claesson-Welsh, Blood vessels as targets in tumor therapy, Ups. J. Med. Sci. 117 (2012) 178–186.
[108] J. Folkman, M. Klagsbrun, J. Sasse, M. Wadzinski, D. Ingber, I. Vlodavsky, A heparin-binding angiogenic protein–basic fibroblast growth factor—is stored within basement membrane, Am. J. Pathol. 130 (1988) 393–400.
[109] G. Bergers, S. Song, N. Meyer-Morse, E. Bergsland, D. Hanahan, Benefits of targeting both pericytes and endothelial cells in the tumor vasculature with kinase inhibitors, J. Clin. Invest. 111 (2003) 1287–1295.
[110] E. Winer, J. Gralow, L. Diller, B. Karlan, P. Loehrer, L. Pierce, et al., Clinical cancer advances 2008: major research advances in cancer treatment, prevention, and screening—a report from the American Society of Clinical Oncology, J. Clin. Oncol. 27 (3070) (2009) 812–826 (Erratum in: J. Clin. Oncol. 2009;27:3070-1).
[111] R. Roskoski Jr., Guidelines for preparing color figures for everyone including the colorblind, Pharmacol. Res. 119 (2017) 240–241.